理學碩士 學位 論文

Surface-Enhanced Raman Scattering with Gold Nanoparticles : From Fundamental to Improvement

(금 나노 입자를 활용한 표면증강라만산란 : 기초와 응용)

蔚 山 大 學 校 大 學 院

化 學 科

徐 旼 廷

Surface-Enhanced Raman Scattering

with Gold Nanoparticles

: From Fundamental to Improvement

指 導 敎 授 하 지 원

이 論文을 理學碩士 學位 論文으로 제출함

2019年 2月

蔚 山 大 學 校 大 學 院

化 學 科

徐 旼 廷

徐 旼 廷의 理學碩士 學位 論文을 認准함

審査委員　　하 지 원　　印

審査委員　　이 영 일　　印

審査委員　　김 용 수　　印

蔚 山 大 學 校 大 學 院

2019年 2月

국문요약

1973년 거친 은 표면에 부착된 피리딘의 라만 신호가 크게 증강되면서 처음 발견된 표면증강라만산란은 신호가 약하다는 라만 분광법의 단점을 보완할 수 있는 유용한 기술이다. 이 기술은 시료의 제약이 거의 없어 미량이거나 수용액 상태에서 분석이 가능하며 비파괴적인 방법으로 생물학적 시료 분석에도 유리하다. 표면증강라만산란은 다양한 분야에 적용 가능함과 함께 라만 분광법의 응용 범위를 확대시키며 활발히 연구되어 오고 있다.

본 연구에서는 금 나노 입자를 적용한 표면증강라만산란의 기초 연구와 메커니즘 연구, 응용 연구를 포함하고 있다. 기초 연구에서는 성게 모양의 뾰족한 팁이 있는 금 나노 입자와 로다민 6G를 이용하여 표면증강라만산란에 영향을 주는 반응 시간, 물질 간의 비율, 원심 분리 정도, 교반 정도 등의 요인들을 각각 조절하여 최적화하는 조건을 찾으며 각 인자들이 의미하는 바를 연구하였다. 다음으로 표면증강라만산란의 유력한 상호 보완적인 두가지의 메커니즘 중 화학적 요인에 초점을 맞추어 전자 당기는 힘이 강할수록 화학적 요인의 기반인 전하 이동이 촉진된다는 가정을 하게 되었다. 금 나노 입자와 친전자성에 따른 작용기를 파라 위치에 치환된 싸이오페놀 유도체를 이용한 메커니즘 연구 결과, 전자를 끄는 기는 전하 이동이 촉진되지만 전자를 주는 기는

분자간 상호작용, 용매 효과 등과 같은 다른 요인을 고려하는 복잡한 접근이 필요하였다. 마지막으로, 금속 표면과 상호작용하지 않거나 안정성이 부족한 분자를 표면증강라만산란에 적용하기 위해 초분자를 도입하여 응용 연구를 진행하였다. 호스트-게스트 상호 작용을 통해 내부가 비어 있는 구조의 초분자에 목표 분자를 넣고 초분자를 이용하여 금속 표면과 상호작용한 결과, 신호 증강이 약 20일 동안 유지되는 것을 확인하였다. 본 연구를 통해 표면증강라만산란에 영향을 주는 인자와 메커니즘에 대한 보다 깊은 이해와 정보를 제공하고 초분자의 도입으로 표면증강라만산란의 더 넓은 범위로의 응용 가능성을 제시하였다.

English Abstract

Discovered from pyridine adsorbed on the roughened silver, surface-enhanced Raman scattering (SERS) has been a useful technique to overcome the main disadvantage of Raman spectroscopy that the signals are weak. SERS has little limitations in sample and enable to analyze very small amounts with high sensitivity or solution sample. Also, this technique is a non-destructive method and advantageous for biological sample analysis. Numerous studies have studied widely to understand this phenomenon, extending Raman spectroscopy and applying for various fields such as plasmonic and chemical sensing in nanoscale.

Herein, basic, mechanism and application research on SERS with gold nanoparticles were conducted. On basic study, we optimized the SERS effect and figured out several factors with gold nanourchins (AuNUs) that had sharp tips and the rhodamine 6G (R6G) as the probe molecules, controlling the parameters individually that were binding time, metal-to-molecule ratio, centrifugation, and stirring that decided the SERS enhancement. Second, the mechanism of SERS, especially chemical enhancement, has been studied with the assumption that electron withdrawing group (EWG) promoted a charge-transfer. Gold nanorods (AuNRs) and thiophenol derivatives substituted with electrophilicity on para-position were used, proving the assumption on EWG but more complicated approaches such as intermolecular interaction and solvent effect were needed on electron donating group (EDG) study. Finally, cucurbit[n]urils (CB[n]), one of useful supramolecular

materials, were used to overcome the limitation of SERS that the adsorbed molecules had to interact with metal surface. By encapsulation of the probe molecules in cucurbit[7]urils (CB[7]) with host-guest interaction and adsorbing CB[7] on surface of AuNRs, the enhanced signal showed a long-term stability for 20 days. These results are helpful to understand deeply SERS, providing information about its principle, mechanism, the factors affecting its enhancement and suggest the potential to utilize SERS on various fields by introducing supramolecular CB[n].

Index

Korean abstract ····· i

English abstract ····· iii

Index ····· v

Scheme index ····· vii

Table index ····· viii

Figure index ····· ix

I. Introduction ····· 1

I-1. SERS ····· 1

I-2. Gold nanoparticles ····· 3

I-3. Cucurbit[n]urils ····· 4

I-4. Objectives of study ····· 5

II. Experimental section ····· 10

II-1. Materials and sample preparation ····· 10

II-1-1. Optimization study for SERS enhancement ····· 10

II-1-2. SERS mechanism focused on chemical effect ····· 10

II-1-3. Application study with cucurbit[7]urils ····· 13

II-2. Instrumentations ····· 13

III. Results and Discussion ····· 16

III-1. Optimization study for SERS enhancement ····· 16

III-1-1. Characterization of gold nanourchins ····· 16

III-1-2. Raman study of rhodamine 6G ····· 19

III-1-3. SERS study with parameters ····· 21

III-2. SERS mechanism study focused on chemical effect ····· 29

III-2-1. Characterization of gold nanorods ····· 29

III-2-2. Benzene ring effect ····· 32

III-2-3. Electron withdrawing group effect ····· 35

III-2-4. Electron donating group effect ····· 41

III-2-5. Enhancement factor calculation ····· 49

III-3. Application study with cucurbit[7]urils ····· 53

III-3-1. The role of cucurbit[7]urils between gold nanorods ····· 53

III-3-2. SERS with long-term stability ····· 56

IV. Conclusion ····· 59

V. Reference ····· 61

Scheme index

Scheme 1. Chemical structure of R6G (A), schematic measurement condition in solution with capillary tube (B) ····· 6

Scheme 2. Representation of adsorbates on gold nanorods (AuNRs) with chemical effect due to the direct charge transfer (A), schematic diagram of SERS measurement with capillary tube and self-assembly monolayers (SAMs) system in sample (B) ····· 8

Scheme 3. Representation of cucurbit[n]urils (CB[n]) and its symbol (A), scheme of formation of aggregation with CB[7] on AuNRs (B) ····· 9

Scheme 4. Classified probe molecules used in this study. Cysteamine and p-ATP for benzene ring effect (pink box), p-ATP, p-MP in case of EDGs (blue box), TP as a standard and p-CTP, p-MBA, p-TFMTP, and p-NTP following the strength of EWGs (green box) ····· 12

Scheme 5. A schematic set-up of backscattering-type confocal Raman spectroscope with a 785 nm laser ····· 15

Scheme 6. Proposed structural forms affected enhancement of EDG molecules. Formation of aggregations through intermolecular interaction, hydrogen bonding between SAMs (A), the effect of solvent, ethanol in ATP and MP (B) ····· 43

Scheme 7. Scheme of two different SERS sample, mixture of AuNRs and R6G (A), AuNRs with encapsulation of R6G in CB[7] (B) ····· 57

Table index

Table 1. Enhancement factors of EWG molecules in common peaks that are C-S vibration in 1090 cm^{-1} and C-C vibration in 1590 cm^{-1} ····· 51

Table 2. Raman and SERS peak assignments for each probe molecule (v : vibration, δ, ɣ : bending, π : wagging) ····· 52

Figure index

Figure 1. A photograph of experimental set-up for Raman spectroscope and microscope. The back side shows the laser source and paths for Raman measurement ····· 15

Figure 2. SEM image (A), TEM image (B) of 100 nm gold nanourchins (AuNUs) ····· 17

Figure 3. UV–Vis extinction spectrum of AuNUs. The dotted-line indicates the wavelength of the incident radiation, 785 nm ····· 18

Figure 4. Raman spectrum of solid R6G (A), normal Raman spectra of R6G solutions at diverse concentrations from 1 mM to 0.5 M (B) ····· 20

Figure 5. SERS spectra with increasing binding time from 0 h to 8 h (A), Raman intensities at 1370 cm−1 obtained from SERS spectra shown in (A), the experimental data were fitted with a linear function (B) ····· 23

Figure 6. SERS spectra at AuNUs concentrations from 0.025 mM to 0.075 mM. Detailed data with more concentrations is provided in Figure 7 (A), Raman intensities at 1370 cm−1 obtained from SERS spectra shown in (A), the experimental data were fitted with a linear function (B) ····· 25

Figure 7. SERS spectra at added AuNUs concentrations from 0.025 mM to 0.4 mM ····· 26

Figure 8. The effect of centrifugation on SERS enhancement ····· 28

Figure 9. The stirring effect on SERS spectra during the binding of the molecules on the metal surface ····· 28

Figure 10. SEM image of AuNRs and a model with the average size 25 nm x 87 nm (A), UV-Vis spectrum of AuNRs showing two distinct LSPR peaks and

the dotted-line indicated a resonance condition with a 785 nm laser (B) ····· 30

Figure 11. Size distributions of AuNRs with gaussian fitting, measured average length 87 nm and width 25 nm. Total 90 particles are counted from SEM images ····· 31

Figure 12. SERS and Raman spectra of cysteamine and ATP for studying the effect of benzene ring ····· 34

Figure 13. Real-time SERS data of NTP from 0 min (after mixing) to 81 min, showing the growth of the distinct peaks (A), the relative Raman and SERS intensities of a peak in 1357 cm^{-1} assigned to NO_2 vibration, finally saturated after about 69 min (B) ····· 37

Figure 14. SERS spectra with EWGs that are TP (A), CTP (B), MBA (C), TFMTP (D), NTP (E) ····· 38

Figure 15. The relative Raman intensities of EWGs spectra with a peak in 1090 cm^{-1}, assigned to C-S vibration. The results show SERS enhancement is proportional to the strength of withdrawing force ····· 39

Figure 16. SERS spectrum of NTP with the lower concentration up to 100 nM, indicating the powerful enhancement ····· 40

Figure 17. SERS spectra with ATP and MP at various concentration (1 mM, 0.1 mM, 0.01 mM) and normal Raman spectrum at 1 mM (A), Raman and SERS signal intensity of the vibrational mode υ(C-S) versus various concentrations (B) ····· 42

Figure 18. UV-Vis spectra of raw AuNRs (red line), NTP adsorbed AuNRs (orange line), MP adsorbed AuNRs (yellow line) and ATP adsorbed AuNRs (green line), showing red-shift with decreasing intensity and weak broadening in case of EDGs ····· 45

Figure 19. DF images of SERS sample with ATP in solution. There are aggregations of AuNRs showing the more intense, brighter and bigger spots in images (A), DF images of SERS sample with NTP in solution. Most signals indicate single particle or small aggregations (B) ····· 46

Figure 20. SERS spectrum of ATP with different solvents that are not capable of proton donation to probe molecules. Standard peaks for the comparison are 1090 cm^{-1} assigned to C-S vibration and 1610 cm^{-1} with C-C vibration. (A), the intensities of SERS standard peaks are plotted with the solvent effect (B) ····· 48

Figure 21. The ideal model of the focal spot of laser and surface area of AuNRs for calculated factors for enhancement factor calculation ····· 50

Figure 22. Photographs of pure AuNRs solution and one with CB[7] (A), SEM images of AuNRs with CB[7] and without CB[7] (B) ····· 54

Figure 23. UV-Vis extinction spectrum of CTAB capped-AuNRs solution (A), centrifugated AuNRs solution (B), AuNRs solution with CB[7] (C) ···· 55

Figure 24. SERS spectra with the time from 6 hours to 20 days without CB[7] (A), with CB[7] (B) ····· 58

I. Introduction

I-1. SERS

Raman spectroscopy has been an important analytical technique that could give information of molecules in vibrational level through the structural fingerprints. Raman spectroscopy can complement the disadvantages of infrared spectroscopy, another analytical vibrational technique, that is hard to obtain clear spectrum in solution state because of the interference of water signals. But Raman spectroscopy also has a fatal disadvantage that the signals are very weak and has a low reproducibility since it is kind of inelastic scattering and the spontaneous scattering is almost 0.0001 % of the radiation. For overcoming this disadvantage of Raman spectroscopy, various techniques have been developed including surface-enhanced Raman scattering (SERS). SERS is the phenomenon can induce a large enhancement of signals by adsorbing the target molecules (called probe molecules or Raman reporters) on the metal surface. The first SERS was discovered from pyridine adsorbed on the roughened silver by Martin Fleischmann etc. in 1973.[1] The magnitude of enhancement of SERS signals compared with normal Raman signals can be represented by the enhancement factor (EF) and the maximum EF of signals published is about ~10^{14}. SERS has shown great advantages of high selectivity, quenching the fluorescence, and the removal of the photodecomposition of molecules.[2-4]

SERS, this simple method to improve Raman spectroscopy, has been considered attractive research topics from fundamentals to applications and studied explosively to this day. For SERS, there are two complementary mechanisms explained about the strong enhancement and proven enough through numerous studies.[5-8] One is the electromagnetic enhancement (EM) that focuses on the surface plasmon resonance of metals, usually plasmonic nanoparticles that feature localized-surface plasmon resonance (LSPR). To be exact, the enhanced electromagnetic field controlled by the roughness or morphologies of metallic nanoparticles is a main reason for the enhancement. As well, the presence of "hot-spot" that is a highly powerful local field created with roughen surface or interparticle spacing between aggregated nanoparticle is the key for the intense signals.[9] There are many efforts to maximize the EM effect developing methods and SERS substrates such as various shapes of nanoparticles, bimetallic systems, nanoparticle on a mirror, controlling a gap size for strong hot-spot, even positioning target molecules on the exact position.[10-14] The other mechanism is the chemical enhancement (CE) related with a charge-transfer between metals and probe molecules. When an adsorbate and metallic nanoparticle form a strong chemical bonding, the metal can act as an intermediate for the excitation of molecules under the condition that the resonance symmetrically between the electric states of molecules and the fermi level of metal.[15-16] Although theorical and experimental approaches have been conducted for revealing the CE, it is relatively less active topic compared with the EM mechanism due to the low contribution on enhancement and has a high potential to find unknown

sections being helpful to elucidate the CE. Because the EM and CE is operative individually but mutually synergizing each unexplainable weak point, the endeavor to understand deeply about each mechanism, especially CE and the relationship should be essential to find out the perfect mechanism for SERS.

I-2. Gold nanoparticles

Gold nanoparticles (AuNPs) are widely used in SERS. For effective SERS, it needs the specific metal that have rough surface or nanostructure, and the plasmonic properties in visible region because the most radiations used in SERS are visible and near-infrared region.[17] So, gold and silver are most commonly used for SERS. AuNPs have high biostability and are easy to synthesize and change the size and the shapes even in nanoscale. Also, AuNPs show a unique phenomenon called localized surface plasmon resonance (LSPR) that is a collective oscillation of free electrons in metal which is high conductive and nano-sized. LSPR depends on the nanoparticle's natures such as sizes, shapes and doesn't be influenced by the surface species.

Gold nanospheres (AuSPs) and gold nanorods (AuNRs) have been studied for SERS commonly due to their simple structures, easy size control and favored adsorptions of the probe molecules on the surface of particles with high surface energy from their facets. AuNRs are anisotropic shaped nanoparticles and its ends of nanorod are sensitive, beneficial for enhanced optical field due to lightning effect.[18]

It is effective SERS substrates in near-infrared (NIR) region that is suitable to decrease the effect of Rayleigh scattering.[17] In addition, a nanorod has 3 different kinds of facets, connected with surface energies and favorable to adsorb molecules effectively on surface, forming stable complexes.[19] Hence, these outstanding properties enable AuNRs appropriate for SERS.

But there haven't studied much about the gold nanouruchins (AuNUs) as the SERS substrate comparatively despite of its high potential. AuNUs are the shape of like sea urchin-shaped nanoparticles that have short and sharp tips around the core and rough surface. Based on the unique shape, we expect the large enhancement with AuNUs because of the larger surface area than the simple, smooth structures and the high sensitivity from the tip effect between the hot-spots.[20-21]

I-3. Cucurbit[n]urils

Cucurbit[n]urils (CB[n]) are promising supramolecular hosts composed of glycoluril repeat units bridged by methylene group as shown in scheme 3A. Compared with other similar molecules such as cyclodextrin, crown ethers, CB[n] has unique properties that have rigid, highly symmetric and macrocyclic pumpkin-shaped structures. Its hollow cyclic structure can allow itself to contain other target molecules inside their hydrophobic cavities through strong host-guest interaction. Furthermore, it can attach on gold surface with identical carbonyl portals leading to

generate uniform, stable sub-nanometer gaps of 0.9 nm, the height of CB[n]. This means CB[n] can induce the powerful hot-spots between AuNP effectively for SERS.[22] Also, the encapsulation inside CB[n] can contribute the improved stability of the structure for SERS and make the enhancement possible without the direct interaction between AuNPs and probe molecules because they enable to interact indirectly through carbonyl portals of CB[n] that places on metal surface due to the trapped state related with EM enhancement.

I-4. Objectives of study

Firstly, we studied about the SERS effect between 100 nm gold nanourchins (AuNUs) as the SERS substrate. These urchin-shaped nanoparticles are hard to control the sizes, numbers and grown sites of the short and sharp tips on the core, the effective adsorption of the probe molecules on the surface are not easy and the following enhancement are not enough. Because the controlling the sub-nanometer gaps (hot-spots) between gold nanoparticles is the most important factor that decide the enhancement. Rhodamine6G (R6G) as shown in scheme 1A was used as probe molecule that is a kind of dye molecules and commonly used for the SERS with AuNPs. It has distinct peaks in Raman spectrum that are convenient for the comparison of the signals. But it has also strong fluorescence signals, we choose a 785 nm diode laser as the radiation that is the near-IR region for the removal of the

fluorescence interference. In addition, a 785 nm wavelength is more beneficial for the R6G molecules following the study about the comparison between 532 nm laser and 785 nm laser on same molecules. So, as shown in scheme 1B, we control the several parameters individually for the optimization of the SERS effect with AuNUs and R6G in this condition that influence the enhancement in system, such as concentrations, binding time, centrifugation for the clear surface and something else during the binding. We didn't consider the temperature and the pH and fix them in all conditions because the temperature could make the shape of the nanoparticle change, the pH effect on R6G was not sensitive.

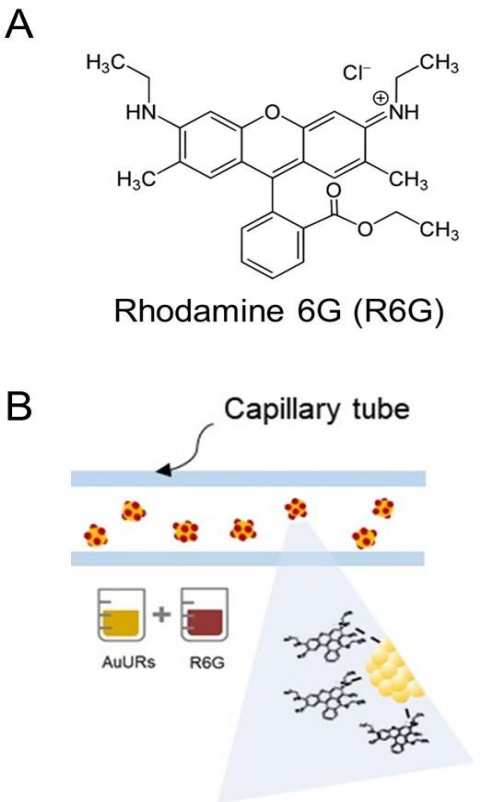

Scheme 1. Chemical structure of R6G (A), schematic measurement condition in solution with capillary tube (B)

Next, we suppose that if molecules with electron withdrawing group (EWG) are binding with gold nanoparticles, more intense and faster enhancement can be possible through the metal-to-molecule charge transfer. Thiophenol derivatives are chosen due to the well-known strong gold-sulfur interaction to satisfy the condition for CE, chemisorption, forming effective self-assembly monolayers (SAMs) on metal surface and the benzene ring amplifying the signal.[23] The benzene ring effect is also studied for demonstrating this system reasonable with cysteamine (Cys) and p-aminothiophenol (ATP) that have same functional groups at each end. Fleger et al. studied para-position showed effectively for SERS than the other position because of a weak steric hindrance.[24] We studied about the SERS effect on para-thiophenol derivatives with different groups containing EWG and electron donating group (EDG) and tried to find the relationship of the chemical charge-transfer and SERS enhancement following the electrophilicity of para-position substituents followed in scheme 2.

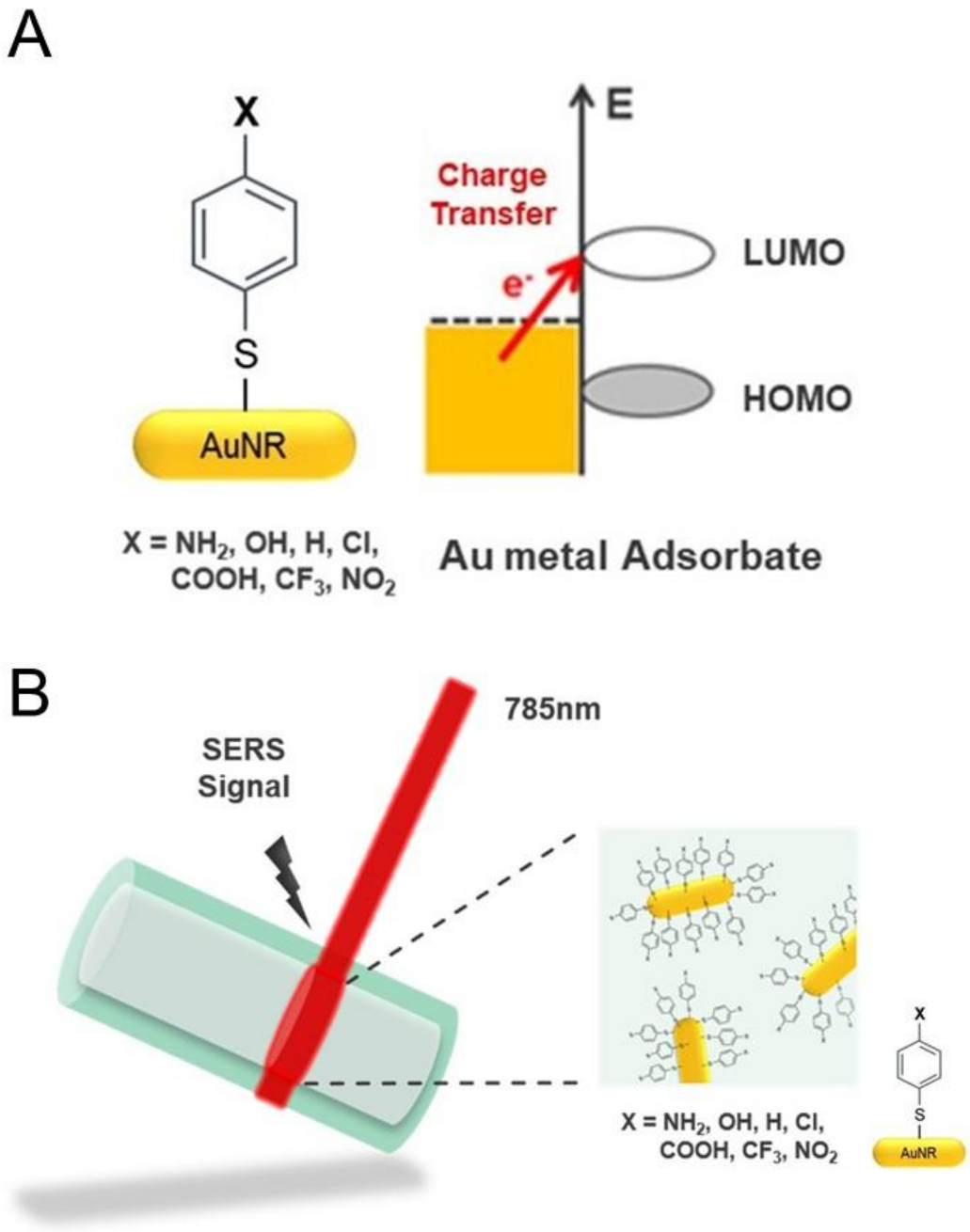

Scheme 2. Representation of adsorbates on gold nanorods (AuNRs) with chemical effect due to the direct charge transfer (A), schematic diagram of SERS measurement with capillary tube and self-assembly monolayers (SAMs) system in sample (B)

Finally, we attempted to introduce CB[7] to overcome the limitation of SERS that unspecific molecules, had weak interaction or low stability with gold surface, are hard to utilize SERS. We tried to make stable aggregations of AuNRs using CB[7] for regular alignments to convince the role of CB[7] and the interaction between AuNRs and CB[7] as shown in scheme 3B. Moreover, we performed SERS study using AuNRs, R6G as probe molecules, and CB[7] focused on stability of these system. CB[7] allowed to achieve a stable encapsulation of R6G in the cavity of CB[7], which was verified by the stable signal in the SERS study.

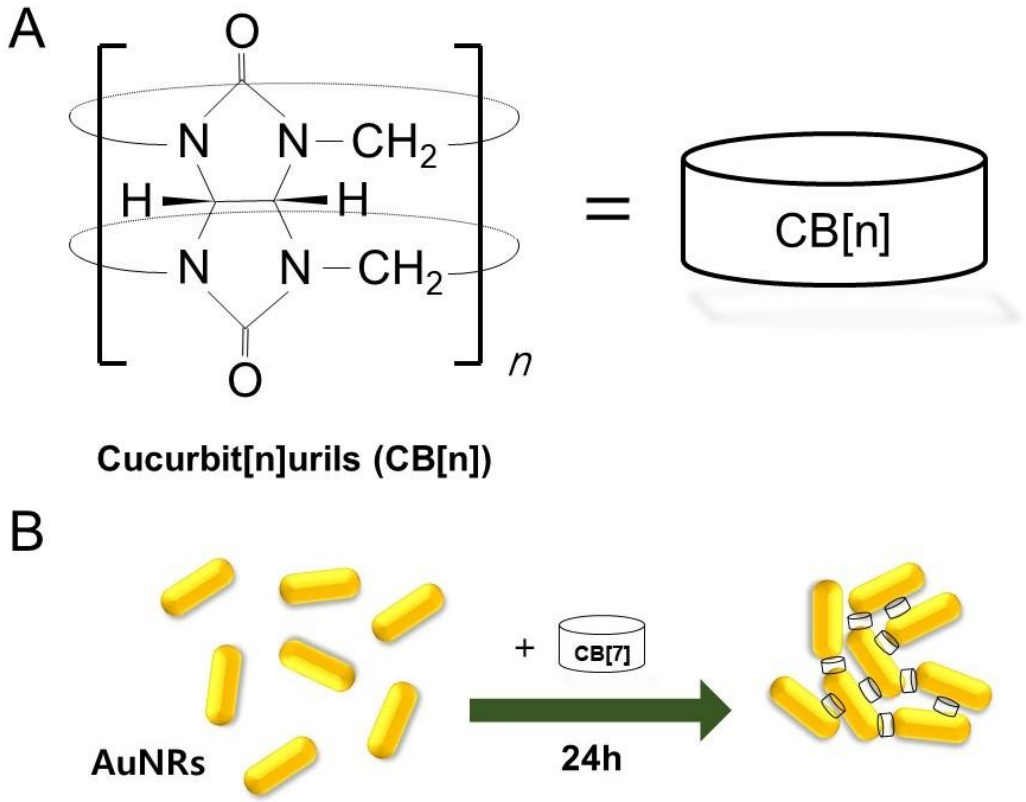

Scheme 3. Representation of cucurbit[n]urils (CB[n]) and its symbol (A), scheme of formation of aggregation with CB[7] on AuNRs (B)

II. Experimental section

II-1. Materials and sample preparation

II-1-1. Optimization study for SERS enhancement

AuNUs with an average size of 100 nm were obtained from Sigma-Aldrich (St. Louis, MO, USA). R6G was purchased from Sigma-Aldrich (St. Louis, MO, USA). Surfactant-stabilized AuNUs solutions were centrifuged at several conditions, but primarily at 2400 relative centrifugal force (rcf) for 40 min and R6G solutions were made with 18.2-MΩ pure water at the proper concentration for each measurement. The SERS samples were prepared as colloidal mixtures of centrifuged AuNUs solutions combined with aqueous solutions of the probe molecule. They were sonicated for a few minutes for mixing and stayed as colloidal mixtures for several hours at room temperature. The prepared samples were put into capillary tubes that were 0.25 mm in diameter and 100 mm in length.

II-1-2. SERS mechanism focused on chemical effect

Cetyltrimethylammonium bromide (CTAB)-stabilized AuNRs (25 nm x 87 nm) used for SERS substrate were purchased from Nanopartz (Loveland, CO, USA).

Probe molecules including cysteamine, p-aminothiophenol (ATP), p-mercaptophenol (MP), thiophenol (TP), p-chlorothiphenol (CTP), p-mercaptobenzoic acid (MBA), p-trifluoromethyl thiophenol (TFMTP) and p-nitrothiophenol (NTP) were obtained from Sigma-Aldrich ((St. Louis, MO, USA). These probe molecules are classified in scheme 4. Ethanol was used for most experiments as solvent, but only cysteamine solution was made with 18.2-MΩ pure water because of the solubility and these solution samples were used for normal Raman measurement.

For SERS sample preparation, 100 μL aliquot of sample was transferred into centrifuge tube from AuNRs (25 nm x 87 nm) stock solution and centrifugated at 12,000 rpm for 10 min for removing surfactant, CTAB. The rinsed AuNRs sample was dispersed in ethanol and added the probe molecules solutions concentrated properly. This colloidal solution was sonicated for a few minutes for enough mixing and stayed about 6 hours for effective binding at room temperature. The prepared samples were put into the capillary tube with the size of 0.25 mm wall, 100mm length.

In case of real-time experiment, 1 mM NTP and AuNRs in ethanol were used with the sample method like SERS sample preparation. As soon as mixing two solutions, it was measured within capillary tube and repeated every 3 minutes until the signal saturated. Each end of capillary tube was sealed for preventing the loss of solvent due to evaporation.

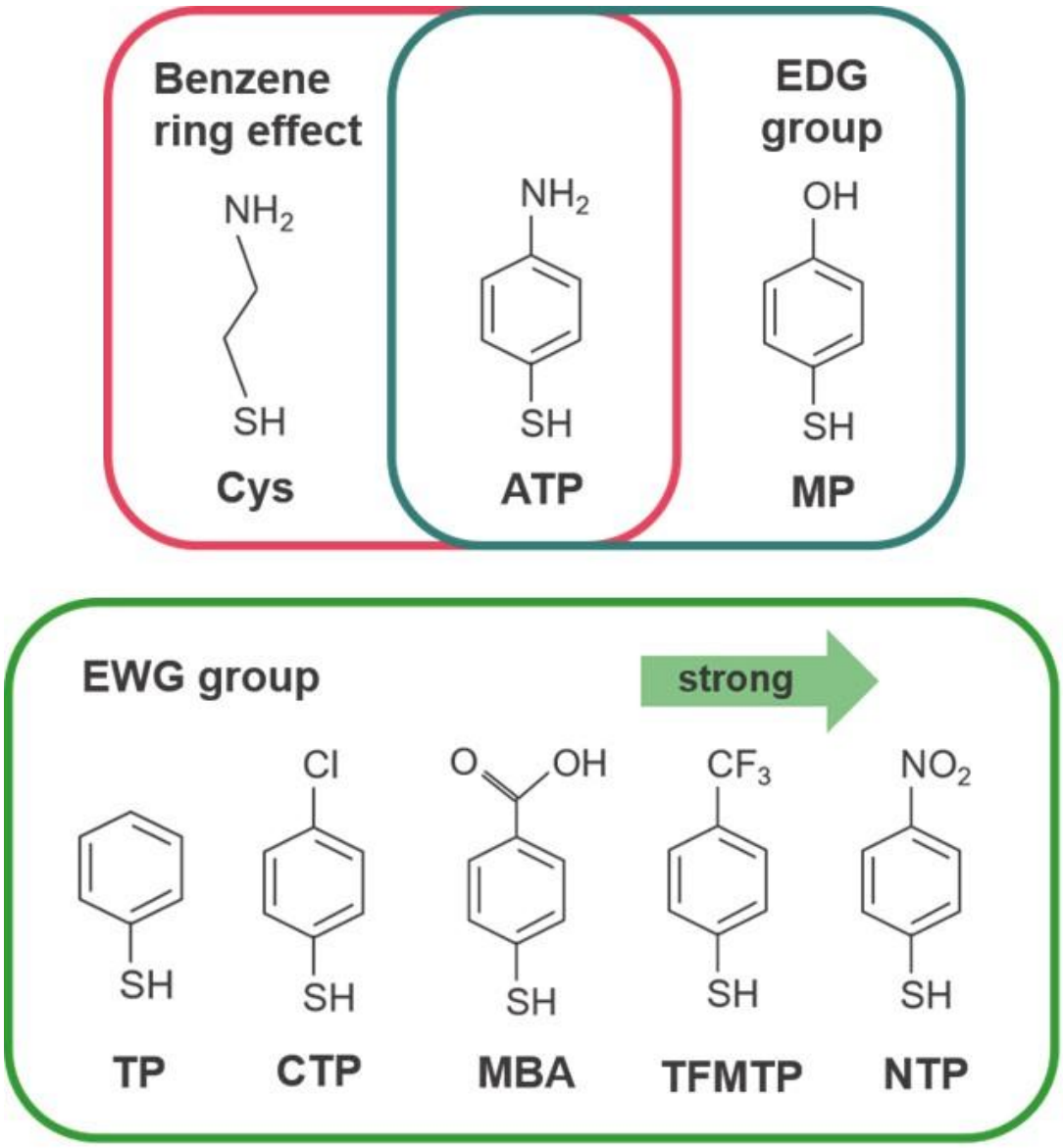

Scheme 4. Classified probe molecules used in this study. Cysteamine and p-ATP for benzene ring effect (pink box), p-ATP, p-MP in case of EDGs (blue box), TP as a standard and p-CTP, p-MBA, p-TFMTP, and p-NTP following the strength of EWGs (green box)

II-1-3. Application study with cucurbit[7]urils

CTAB-stabilized AuNRs (25 nm x 73 nm) used for SERS substrate were purchased from Nanopartz (Loveland, CO, USA). CB[7] was synthesized by Prof. Kimoon Kim in Postech. For the bulk sample, 400 μL of 1 mM CB[7] in water was added to 4 mL AuNRs solution and raw AuNRs solution was used as control sample. Two samples were prepared for SERS experiment. One was 100 μL AuNRs solution and 100 μL of 1 mM R6G molecules and the other was 100 μL AuNRs solution with encapsulated R6G inside CB[7] cavity. The amounts and concentrations of CB[7] and R6G solution in two different samples fixed identically for the effective comparison. In encapsulation sample, the molar ratio of CB[7] and R6G was 1:1 because CB[7] can contain one molecule inside the cavity. These two samples were measured respectively after 6 hours, 1 day, 8 days, 20 days for the long-term stability on room temperature.

II-2. Instrumentations

The shape and the size of AuNPs were characterized with a scanning electron microscope (SEM) (Jeol, Tokyo, Japan). UV–Vis extinction spectra were collected in a quartz absorption cell with a Varian Cary 300 UV–Vis

spectrophotometer (Agilent, CA, USA). For UV–Vis measurements, bare AuNPs solutions were used without any dilution. DF scattering microscopy was carried out under a Nikon inverted microscope (ECLIPSE Ti-U, JAPAN) in this study. In DF mode, we utilized a Nikon Plan Fluor 100× 0.5–1.3 oil iris objective and a Nikon DF condenser. We used an Andor iXonEM+ CCD camera (iXon Ultra 897, UK) to obtain DF scattering images of AuNPs. The collected images were analyzed with the program, Image J.

A custom-made Raman spectroscopy system with a 785 nm diode laser (Thorlabs, Newton, NJ, USA) was used for the Raman and SERS measurements. The schematic and real instrument were presented in scheme 5, figure 1. The capillary tubes with the samples were placed onto the microscope stage, and the laser power was set to ~60 mW. However, the real power that arrived at the sample was about half of the initial power due to the loss by the path and mirrors. The monochromator with the spectral resolution of 0.1 nm was used with 600 I/mm grating and the slit width was about 100 μm. The Raman spectra were collected with 40 X objective lens that had numerical aperture, 0.75. and an Andor spectrometer (SHAMROCK 303i, UK) connected to an Andor CCD camera (Newton Du 9209-OE, UK). All the spectra were obtained and analyzed with the Matlab R2016b program.

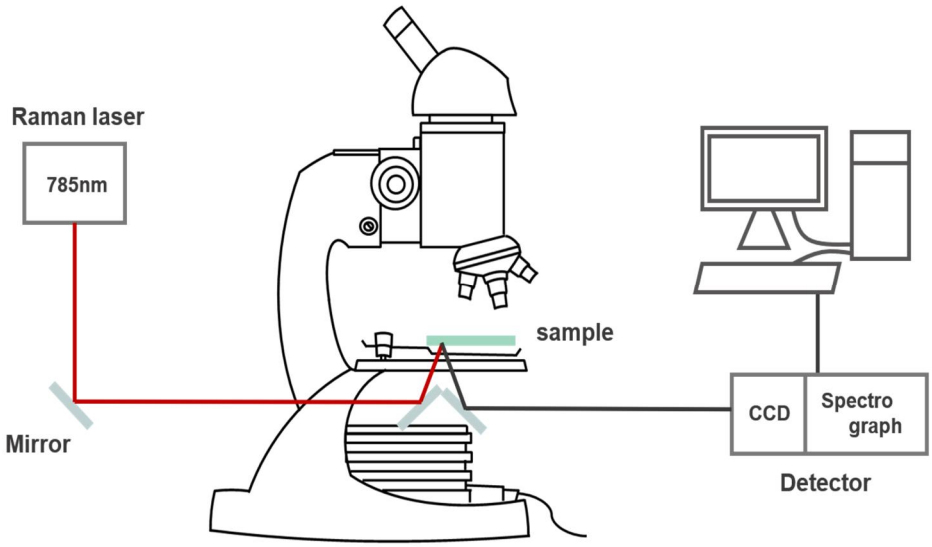

Scheme 5. A schematic set-up of backscattering-type confocal Raman spectroscope with a 785 nm laser

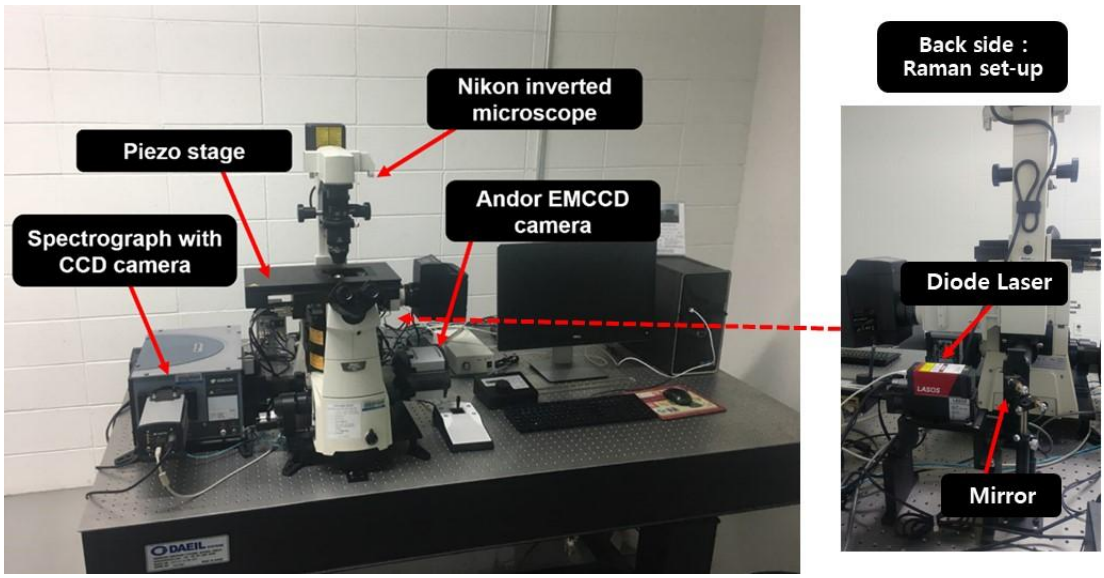

Figure 1. A photograph of experimental set-up for Raman spectroscope and microscope. The back side shows the laser source and paths for Raman measurement

III. Results and Discussion

III-1. Optimization study for SERS enhancement

III-1-1. Characterization of gold nanourchins

We first characterized the shapes and sizes of AuNUs used as SERS substrates. As shown in SEM and TEM image of figure 2, 100 nm AuNUs had sharp and relatively shorter tips than gold nanospheres (AuSPs). Furthermore, the AuNUs were almost identical in size and shape. However, the locations and numbers of their tips and the roughness were distributed randomly about the core. We then measured the UV–Vis extinction spectrum of the AuNUs with a Varian Cary 300 UV–Vis spectrophotometer, as shown in figure 3. The spectrum had a single broad LSPR peak at around 676 nm, which differed from that of AuSPs with multiple LSPR peaks. As seen in figure 3, the LSPR peak of the AuNUs occurred at a 785 nm wavelength (green dotted-line in the spectrum), the laser wavelength used for Raman measurement. This means that there could have been a resonance effect between the gold and the radiation, and that electromagnetically enhanced signals can be expected with 100 nm AuNUs at 785 nm.

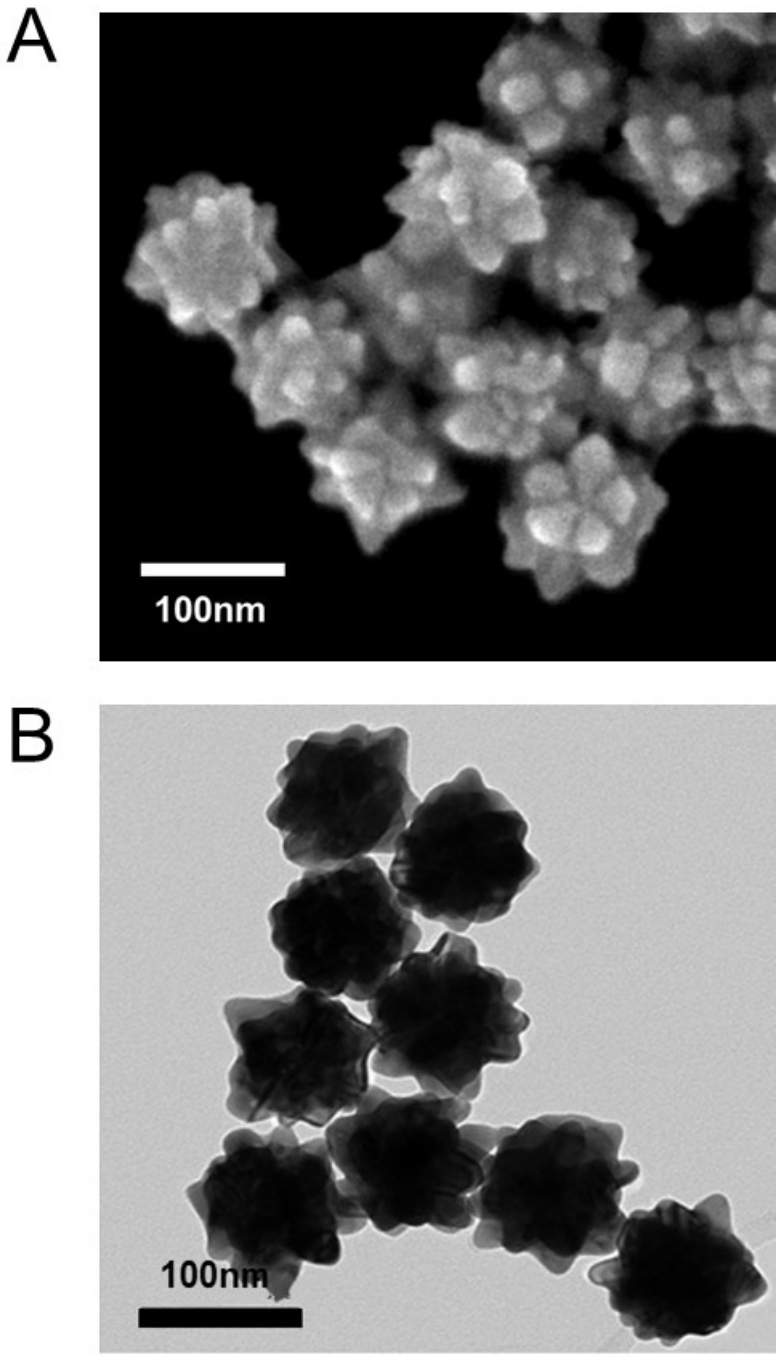

Figure 2. SEM image (A), TEM image (B) of 100 nm gold nanourchins (AuNUs)

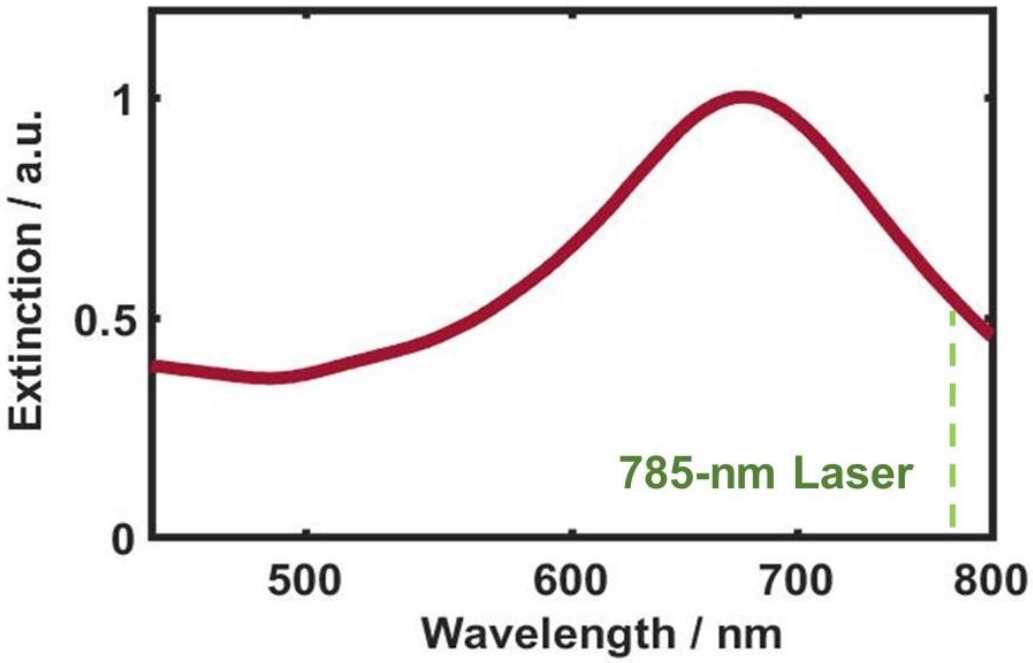

Figure 3. UV–Vis extinction spectrum of AuNUs. The dotted-line indicates the wavelength of the incident radiation, 785 nm

III-1-2. Raman study of rhodamine 6G

We carried out Raman studies using R6G as probe molecules. The experimental set-up for Raman spectroscopy used in this study is depicted in scheme 1 and figure 1. To confirm its distinct Raman signals in a spectrum, we first measured solid R6G molecules as in figure 4A. From the spectrum obtained, the R6G showed its characteristic peaks at 560 cm^{-1}, 774 cm^{-1}, 1185 cm^{-1}, 1311 cm^{-1}, and 1531 cm^{-1}. The Raman band at 560 cm^{-1} indicated the in-plane bending vibration of the aromatic ring in the R6G molecule. The band at 774 cm^{-1} was assigned to the C-H out-of-plane bending vibration, and that at 1311 cm^{-1} as the C-O-C stretching mode. The Raman signals in fingerprint at 1185 cm^{-1} and 1531 cm^{-1} were caused by the symmetric modes of the in-plane C-C stretching vibrations of R6G.[3, 25] The Raman spectra at varying concentrations of R6G solution, ranging from 0.5 M to 1 mM, are shown in figure 4B. The solution samples had little red shift compared to solid samples. However, the distinct peaks of R6G were still evident. The highest concentration of 0.5 M (orange curve) showed a clear spectrum similar to the solid R6G spectrum in figure 4A. However, lowering the concentration of the samples caused a decrease in the signal intensities, and the peaks became unclear and weaker. Even in the lowest concentration of 1 mM (blue curve), it was difficult to identify R6G Raman signals. The spectra had only broad mixed peaks due to poor resolution. Therefore, in this study, we chose the lowest concentration of 1 mM of

R6G solution for the following SERS studies.

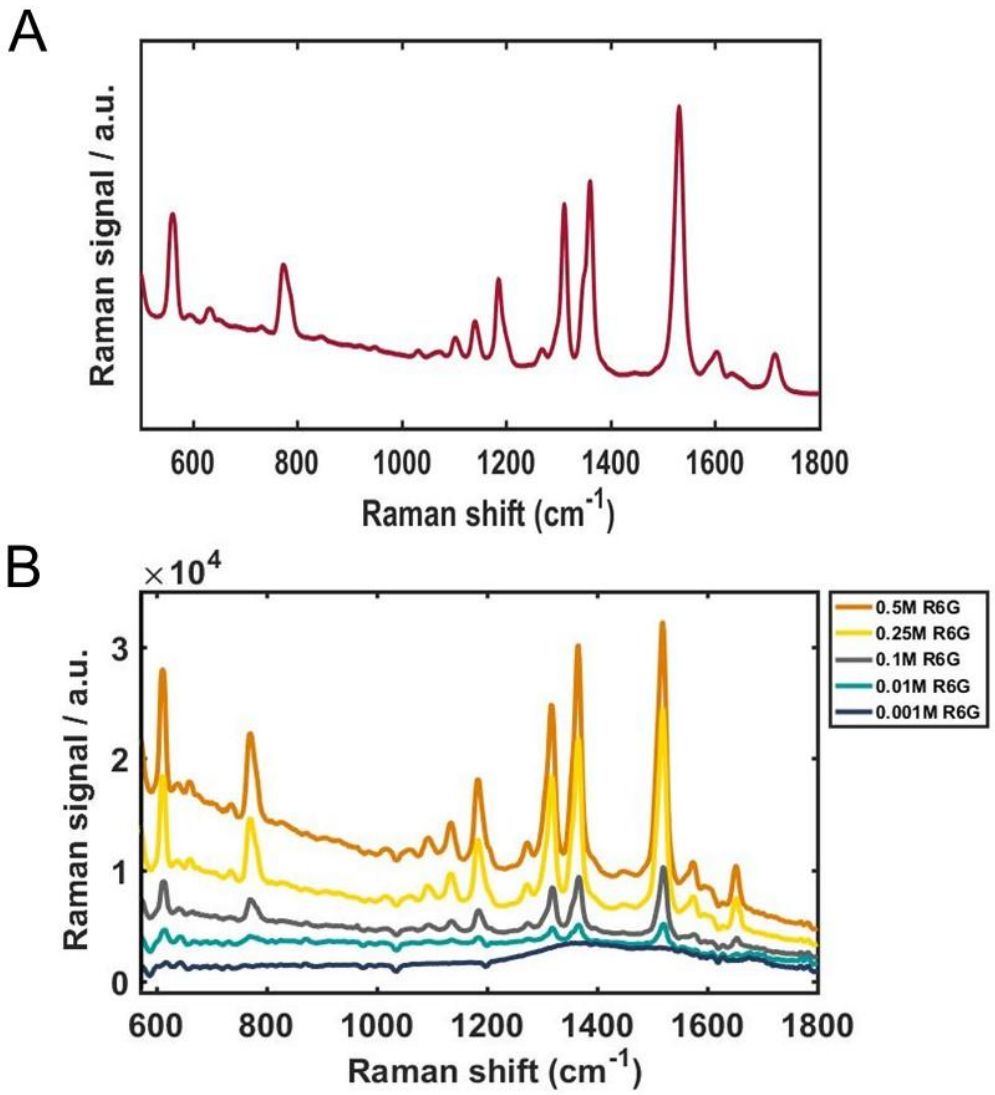

Figure 4. Raman spectrum of solid R6G (A), normal Raman spectra of R6G solutions at diverse concentrations from 1 mM to 0.5 M (B)

III-1-3. SERS study with parameters

AuNUs have great potential in SERS because of their sharp tips and unique optical properties. However, the number of tips, their sizes, and their locations relative to the cores of the AuNUs are hard to control.[26] In addition, it is difficult to achieve the effective adsorption of probe molecules on the rough and tipped surfaces. Because of these factors, it has been doubtful whether they would be good as SERS substrates. In this regard, we attempted to control and optimize several factors that affect the Raman enhancement in AuNUs. In this study, we did not consider temperature and pH and set them as constant in all the conditions because the temperature can affect nanoparticle shape and R6G is not pH sensitive.[27] We first tested the effect of binding time between AuNUs and R6G, one of the important factors for effective SERS. The complete mechanism of SERS has not yet been revealed. However, there are two main mechanisms that have been widely accepted.[28] One is the electromagnetic (EM) effect, and the other is the chemical effect (CE). The EM effect is caused by an amplified EM field generated with superposition of the surface plasmon resonance of the gold nanoparticles. The CE is associated with the electronic coupling of molecules adsorbed on the surface and the charge transfer between the adsorbed analyte and the metal surface. Therefore, the binding time is related to the CE, having direct influence on the enhancement of SERS. We investigated the effective adsorption of R6G molecules at different binding times from 0 h (no binding time) to 8 h at room

temperature shown in figure 5A.[29] For studying only the effect of binding time, we held the other factors constant for each sample. With no binding time, the SERS spectrum was rough and had barely present peaks of R6G, which was similar to the normal Raman data of the probe molecules in 1mM concentration. This means that spontaneous binding did not occur in a few minutes and took at least 2 h. If there were any successful adsorptions, there would be distinct Raman peaks indicative of the enhancement of SERS. The broad bands between 1200 cm^{-1} and 1600 cm^{-1} were caused by the capillary tubes and were not signals of the analytes. As the binding time increased, the enhancements increased, growing clear peaks from the R6G despite the interference of the capillary tubes. When the binding time was 6–8 h, the result was most prominent with the highest resolution, indicating the effective adsorption of molecules on the surface. Figure 5B shows Raman intensities at 1370 cm^{-1} at each condition in figure 5A, fitted with a linear function. As seen in figure 5B, the Raman intensity increased steadily with increasing binding time, and the point at 8 h was slightly off the linear fit line. However, after 8 h, the resolution was undesirable due to the weak interaction between the metals and the probe molecules. R6G with its positive nitrogen site can interact with AuNUs through Van der Waals interactions, not by chemical bonding.[30-31] In the CE, strong interactions lead to a high active SERS. However, the weak interaction between gold and R6G decreased the stability of the attached R6G, hence, the lifetime of this chemical form was shortened.[32] In other words, after a certain period, the R6G molecules could detach from the surface, which caused the decrease in resolution.

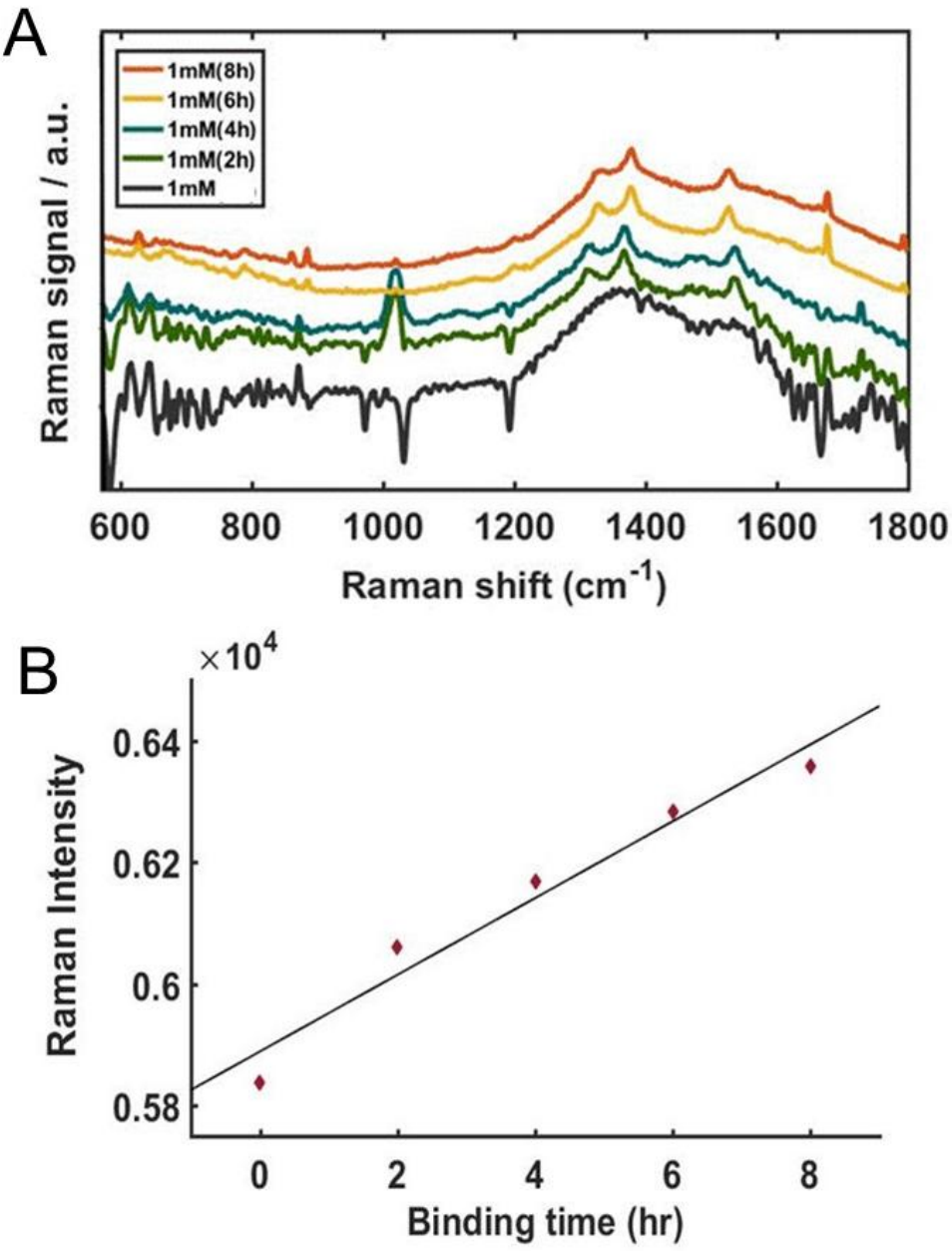

Figure 5. SERS spectra with increasing binding time from 0 h to 8 h (A), Raman intensities at 1370 cm−1 obtained from SERS spectra shown in (A), the experimental data were fitted with a linear function (B)

Next, we investigated the ratio between AuNUs and R6G by controlling metal concentrations while fixing the concentration of the probe molecules. Likewise, other conditions were kept constant during this experiment. We obtained the SERS spectra with 0.025 mM, 0.05 mM, and 0.075 mM of AuNUs while the concentration of R6G solution was fixed to 1 mM. With increasing concentrations of AuNUs, the SERS signals were enhanced noticeably with improved resolution shown in figure 6A. Furthermore, the peaks at 1103 cm^{-1}, 1140 cm^{-1}, and 1197 cm^{-1}, not observed in 0.025 mM, appeared at higher concentrations. For clearer comparison, we fitted the Raman intensities at 1370 cm^{-1} with a linear function as shown in figure 6B, and the experimental data were well fitted by the linear function. We then tried to find the limit for linear response by increasing the concentration continuously in figure 7. From the results, we observed that the Raman signal steadily increased with increasing concentration, and the greatest increase was observed at 0.3 mM (the ratio of metal to molecules was about 8). However, beyond that 0.3 mM concentration, the line collapsed, and the peaks were difficult to distinguish even though the overall spectra increased. This result can be ascribed to the excessive concentrations of metals inducing aggregation, causing the number of molecules participating in SERS to be reduced due to the narrower area of the surface to which the probe molecules could be attached.[33] As a result, the resolution was low because the system failed to have the minimum numbers of molecules required for enhancement. This is a reasonable explanation because we removed the surfactant to prevent the formation of aggregates between gold nanoparticles, which have a high probability of agglomeration.

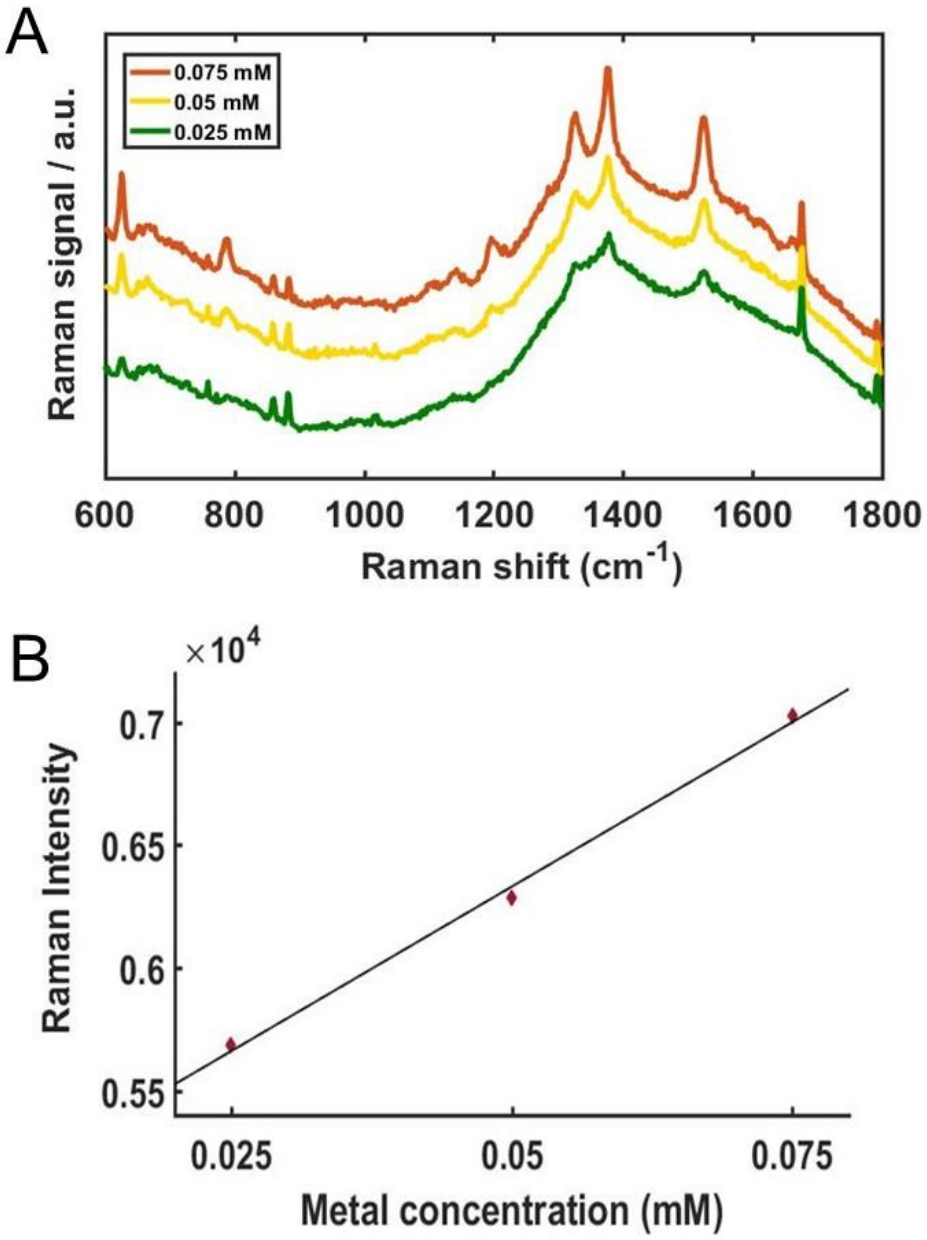

Figure 6. SERS spectra at AuNUs concentrations from 0.025 mM to 0.075 mM. Detailed data with more concentrations is provided in figure 7 (A), Raman intensities at 1370 cm^{-1} obtained from SERS spectra shown in (A). the experimental data were fitted with a linear function (B)

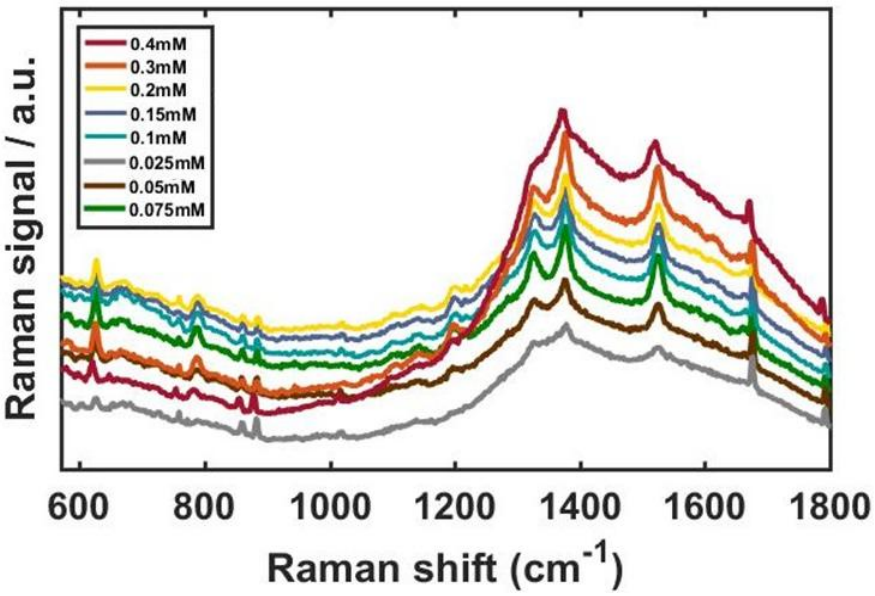

Figure 7. SERS spectra at added AuNUs concentrations from 0.025 mM to 0.4 mM

During the SERS experiments, we noted that the magnitude of Raman enhancement differed slightly with the centrifugation conditions. The centrifugation step was carried out to remove the surfactants that surrounded the AuNUs, thereby minimizing the interference of the effective adsorption of R6G molecules on the particle surface. Because spontaneous desorption of surfactant from the surface is rare, we had to remove it intentionally, and centrifugation was the easiest and simplest method. We used four sets of centrifugation conditions: 2400 rcf for 20 min, 40 min and 4800 rcf for 20 min, 40 min. As shown in figure 8, centrifugation at 2400 rcf for 40 min showed greater enhancement for 100 nm AuNUs than did another centrifugation condition. This result means that the condition of 2400 rcf for 40 min can remove the surfactants from the surface more effectively so that the R6G

molecules can be more conveniently attached to the empty surface, resulting in the higher enhancement of SERS. Therefore, the centrifugation step has to be considered for effective SERS experiments and large Raman enhancement. In addition to the aforementioned centrifugation effect, we further investigated the stirring effect on SERS. Most sample preparation for SERS contained a stirring step for fast, complete adsorption in the system. With stirring, the adsorption time could be shortened, and the molecules could be attached more strongly to the metal surface, with additional energy generated from stirring of the samples. In the present study, we set the total binding time to 6–8 h and evaluated five different stirring times, from 0 h (meaning no stirring step) to 4 h. As shown in figure 9, we noticed that the longer stirring time degraded the intensity as well as the resolution. The spectrum of the sample stirred for 4 h rarely had peaks and showed the lowest intensities compared with other conditions. The red curve in figure 9, from the sample with no stirring, showed the distinct Raman peaks of R6G. The result can be explained by weak Van der Waals interactions between the R6G molecules and the AuNUs, not by chemical bonding. This interaction can be influenced by a physical force such as stirring, and continuous stirring can easily interrupt the binding or remove any instances of weak binding. Therefore, we concluded that it is favored not to have a stirring step in sample preparations for SERS experiments using AuNUs and R6G molecules.

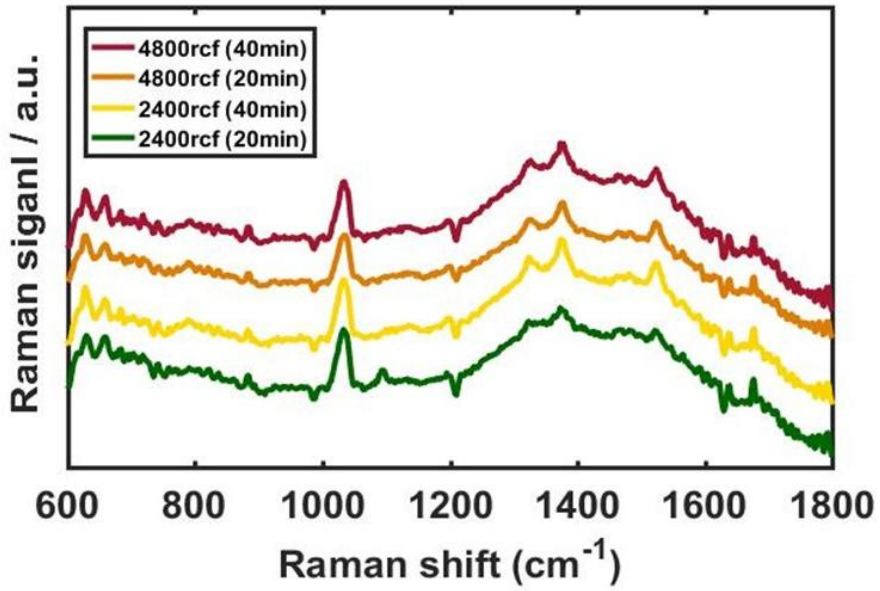

Figure 8. The effect of centrifugation on SERS enhancement

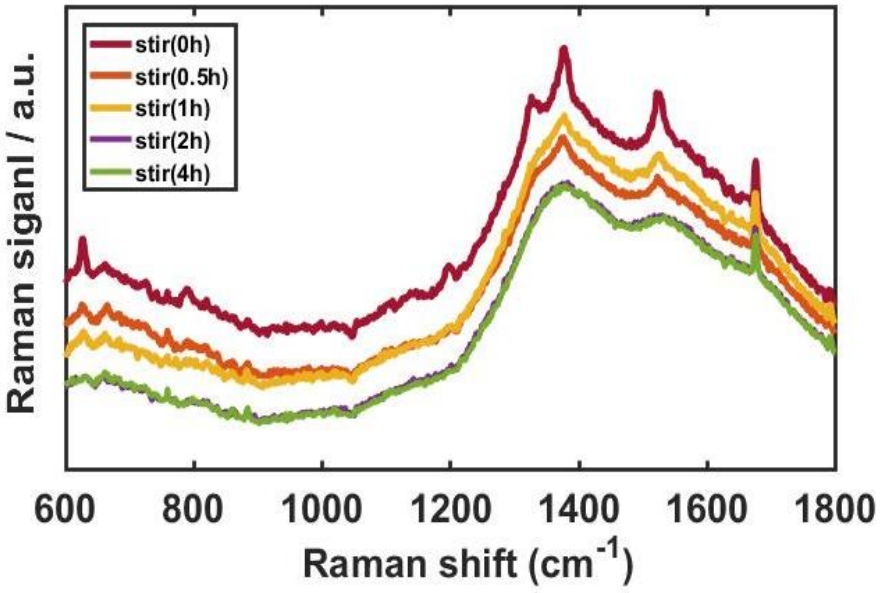

Figure 9. The stirring effect on SERS spectra during the binding of the molecules on the metal surface

III-2. SERS mechanism study focused on chemical effect

III-2-1. Characterization of gold nanorods

AuNRs have an anisotropic shape and unique optical properties, unlike nanosphere. Figure 10A shows the identical shape and size of nanoparticles characterized by the SEM images and the size distribution data and additional SEM image are provided in figure 11 with the mean value, 86.94 (± 5.28) nm x 25.37 (± 2.48) nm and an aspect ratio as 3.5. The UV-Vis extinction spectrum of AuNRs in figure 10B indicates two localized surface plasmon resonance (LSPR) peaks derived from the shape effect. The left peak at 520 nm is a transverse mode generated with the short axis and the right one in NIR region, 776 nm is a longitudinal mode from the long axis of nanoparticles known as more sensitive.[34-35] As abovementioned and designed by self-assembly monolayers (SAMs) probes from scheme 2, the dashed line near the LPSR longitudinal peak in figure 10B indicates that the laser power wavelength was set close to 770 nm. The latter enabled large hot electron populations to be transferred from AuNRs to probes molecules and favor a high probability of direct hot electrons transfer processes. Therefore, a resonance effect between longitudinal LSPR peak of AuNRs and a laser wavelength of 785 nm is expected in this study.

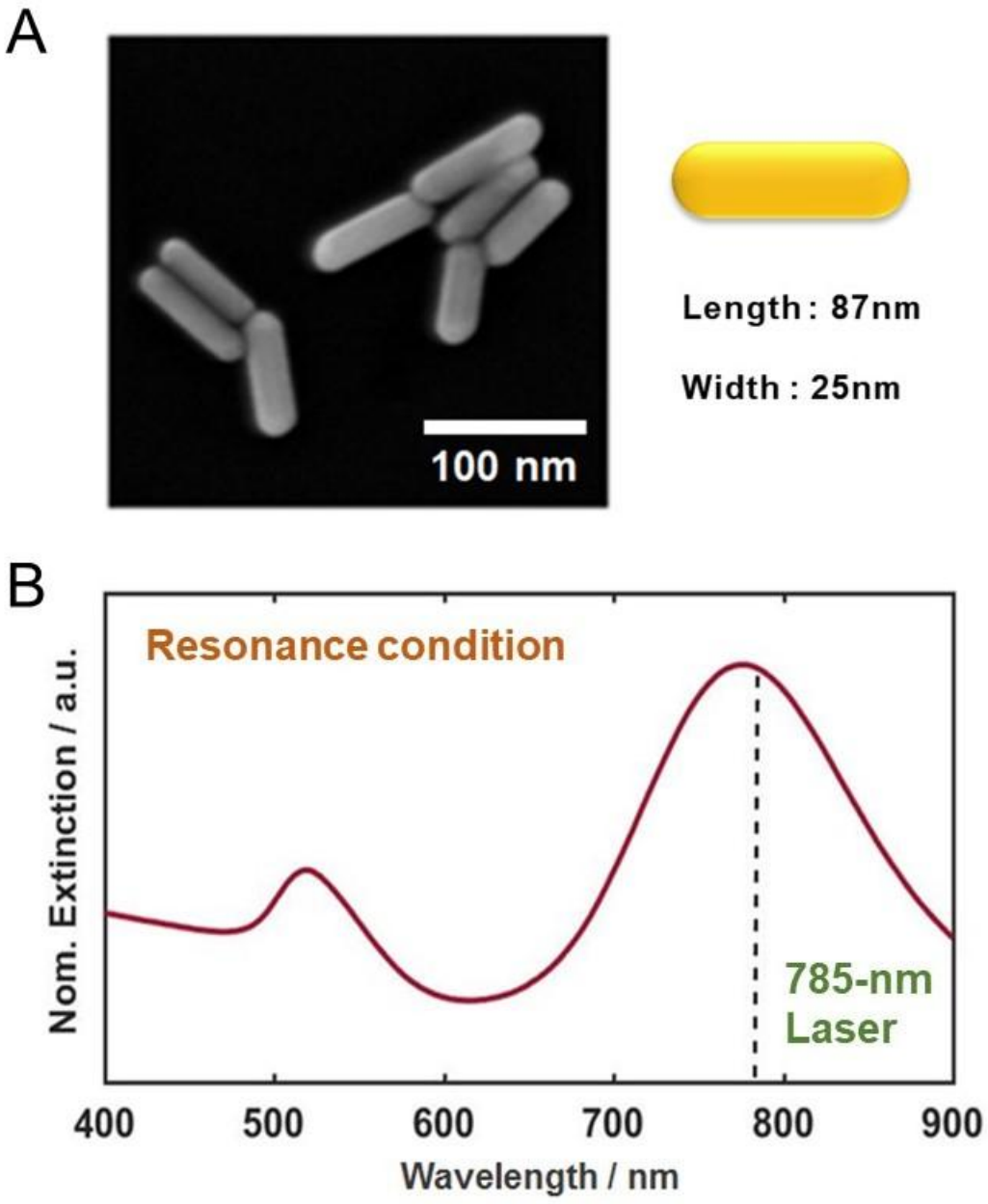

Figure 10. SEM image of AuNRs and a model with the average size 25 nm X 87 nm (A). UV-Vis spectrum of AuNRs showing two distinct LSPR peaks and the dotted-line indicated a resonance condition with a 785 nm laser (B)

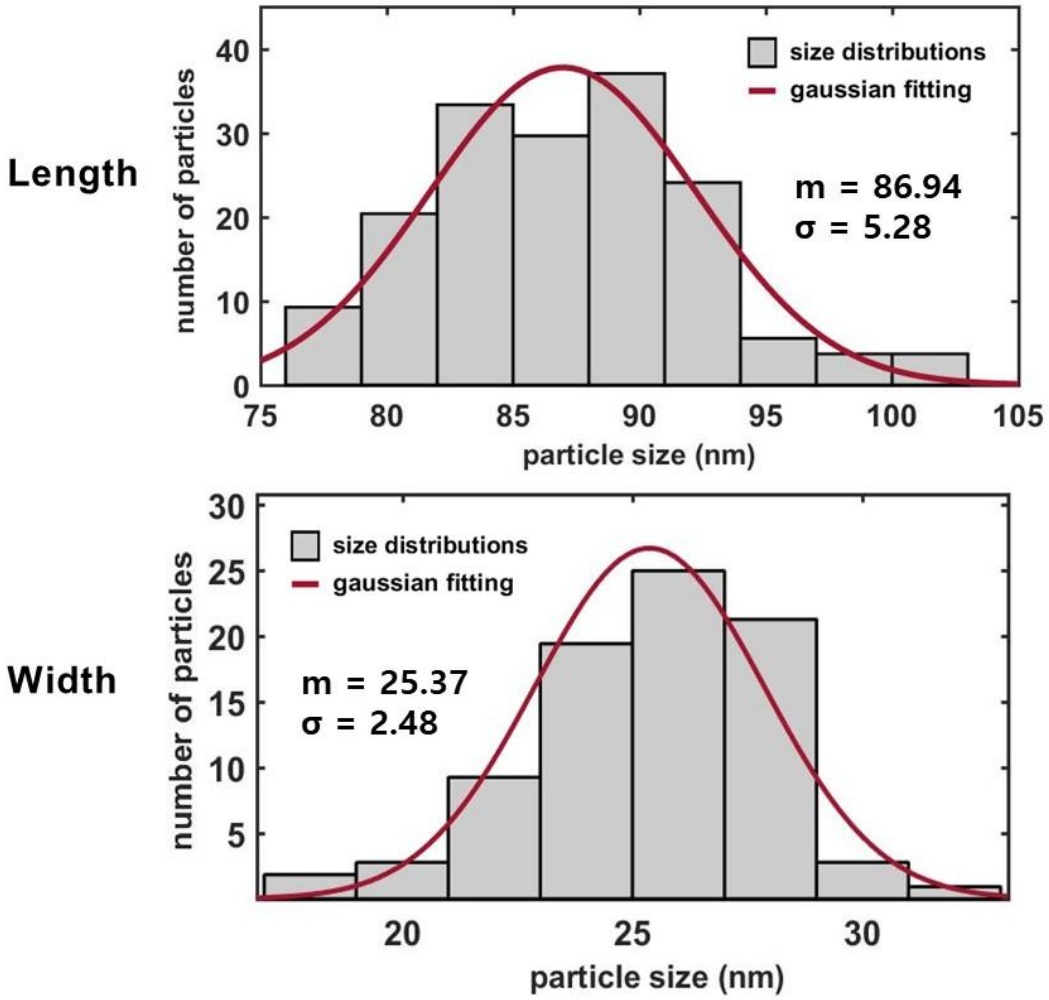

Figure 11. Size distributions of AuNRs with gaussian fitting, measured average length 87 nm and width 25 nm. Total 90 particles are counted from SEM images

In fact, the case used off-resonance condition has been dominated for excluding the EM effect at most, concentrated with pure CE. However, we are willing to use the resonance condition because the EM effect has been identified as a main contribution toward enhancement.[15] When the EM effect got weakened by non-resonance condition, the magnitude of enhancement might damage with weak results

and low reproducibility. Even the spontaneous self-assembly monolayer system, not exquisitely-designed substrates for extreme enhancements, like our condition could go through troubles in obtaining enough data for effective comparison. For optimizing this experiment, we control the all factors influenced in EM effect with same condition and has gotten a same EM effect expecting high enhancement but focusing CE well.

III-2-2. Benzene ring effect

Firstly, we explore about the effect of the presence of the conjugation system, like aromatic ring in SERS. Cysteamine and ATP have two identical functional ending groups, amine ($-NH_2$), thiol (-SH) at each end, linking by carbon chain, benzene ring, respectively as shown in scheme 4. Each molecule has similar molecular size and structure, aminothiol-based hydrocarbon so that it is reasonable to compare the effect of benzene ring. In figure 12, the SERS spectra of cysteamine and ATP indicates cysteamine shows certainly low enhancement even though the 100 times higher concentration than ATP solution. Also, carbon chain can be flexible, contrary to rigid benzene ring causing the gold-amine interaction through bending. It is possible cysteamine to interact with gold surface as two kinds that is trans and gauche conformation.[18] Trans conformer formed a bonding with only thiol group, whereas both functional group interact with gold surface, called gauche conformer. The presence of these two conformers were demonstrated with the peak in 660 cm^{-1}

corresponding with gauche form and 740 cm^{-1} with trans form.[6] The gauche form means the possibility of higher enhancement due to the strong interaction with gold surface and getting close to surface due to stronger EM effect, but the opposite result is not in accordance with this approach and the higher signals of ATP can be explained only with the difference between molecular structure, resonance hybrid benzene ring.[36] Benzene ring has a planar delocalized structure with free pi electrons, compared with restricted sigma bonding of carbon chains. This means six carbons in benzene can share electrons equally and beneficial for fast and active electron flow resulting higher SERS enhancement. In addition, all thiophenol derivatives show the more intense signals than cysteamine suggesting the evident contribution of benzene ring on SERS enhancement with the following results. It is no doubtful benzene ring to amplify the signals successfully due to its structural properties.

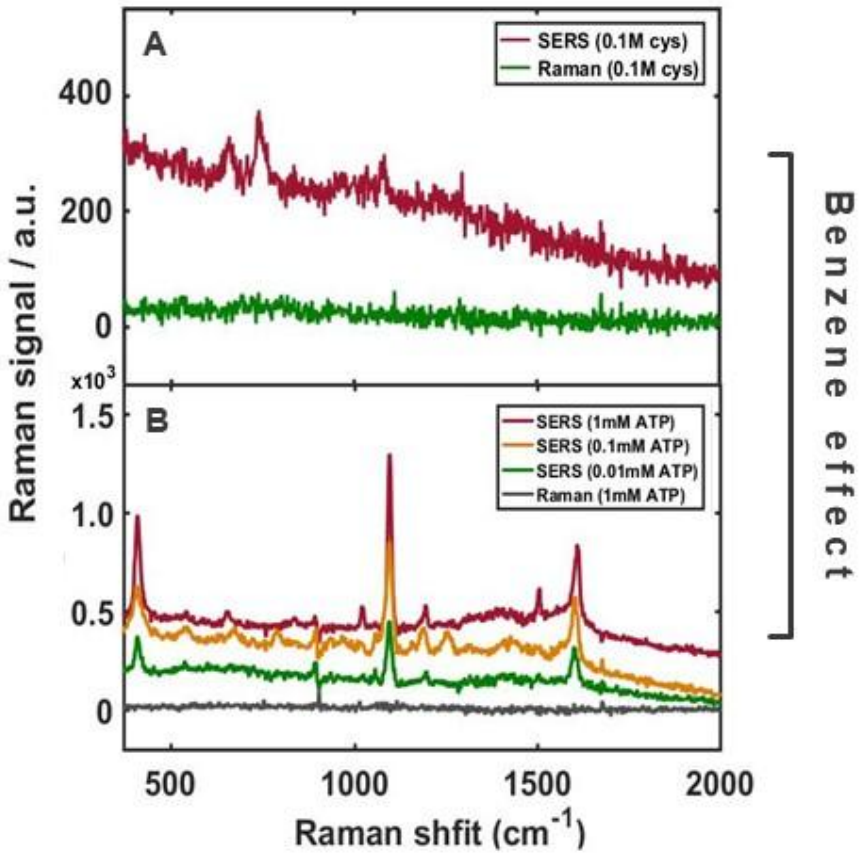

Figure 12. SERS and Raman spectra of cysteamine and ATP for studying the effect of benzene ring

III-2-3. Electron withdrawing group effect

We study about the substitution effect when they are all EWGs, set TP with only hydrogen as a standard and select four samples following the strength of EWG behavior, CTP (chloro-), MBA (carboxylic-), TFMTP (trifluoro-), NTP (nitro-). All the samples contained thiophenol structure for the effective binding with AuNRs by a strong gold-sulfur interaction and the signal amplification by benzene ring. The effective binding of probe molecules is demonstrated with the real-time SERS experiment with NTP as shown in figure 13. After 69 minutes, the enhanced signals of standard peak assigned NO_2 peak are saturated indicating densely packing on gold surface. In figure 14, SERS spectra of each sample showed a common highly enhanced peak around 1090 cm^{-1} assigned to C-S vibration, demonstrated both the chemical binding between molecules and metal surface and a charge transfer occurred through thiol group, sulfur atom. The plotting graph of the relative intensities of this peak representing C-S vibration shown in Figure 15 indicates the increasing intensities depending on the strength of EWG. Also, another common intensity of the signal near 1590 cm^{-1} corresponded C-C ring vibration indicates the benzene ring causes the improvement in signals and charge travels around them certainly and this peak is related with "b_2 mode" known as the symbol for the presence of CE mechanism.[37-38] The calculated enhancement factor of both C-S vibration and C-C ring vibration in table 1 support this result has enough tendency following the functional group fitted well with our assumption. Because the para-

position functional groups were much far from the surface than benzene or thiol part, the enhancement could be rather weak due to weak coupling with surface plasmon resonance (SPR). Hence, when the molecule endured small enhancement, the functional peak could not be appeared or weak relatively in spectrum. As shown in Figure 14, we could notice the peak of functional groups become larger when the functional group was stronger EWGs at 560 cm^{-1} of CTP, 896 cm^{-1} of MBA, 407 cm^{-1} of TFMT and 1126 cm^{-1}, 1357 cm^{-1} of NTP. Even NTP showed a peak in 1357 cm^{-1} assigned nitro group ($-NO_2$), the highest peak in spectrum, over C-S vibration and large enhancement up to 100 nM as shown in figure 16. The rest molecules showed C-S vibration was almost overwhelming than other vibrations. As well, peaks corresponding b_2 mode appeared gradually showing the connection with CE effect and results when the molecules had stronger EWG in structure and this means there is no doubt to be tied relationship up between the results and charge transfer of the adsorbed molecules on metal, not mainly EM effect.

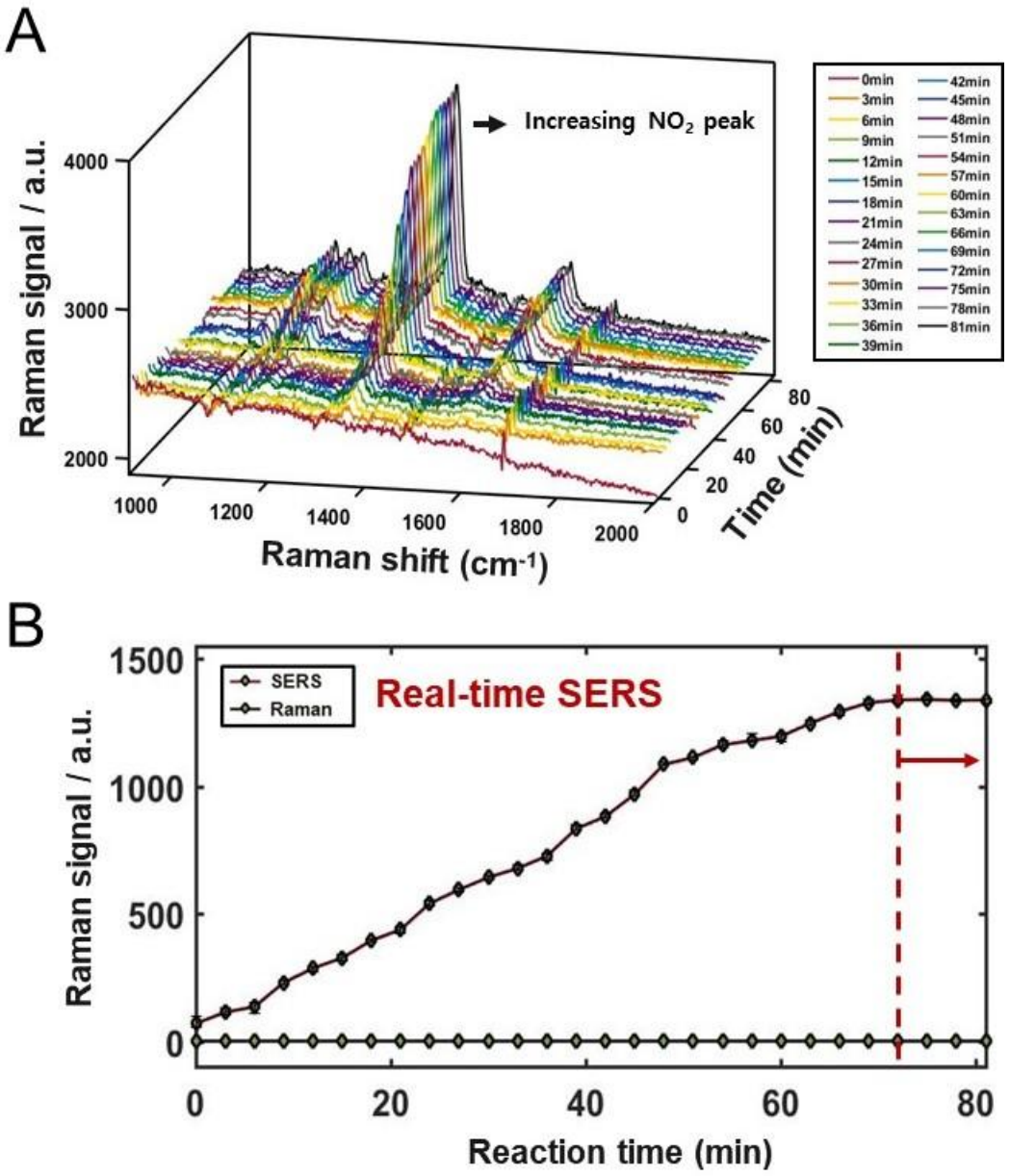

Figure 13. Real-time SERS data of NTP from 0 min (after mixing) to 81 min, showing the growth of the distinct peaks (A), the relative Raman and SERS intensities of a peak in 1357 cm^{-1} assigned to NO_2 vibration, finally saturated after about 69 min (B)

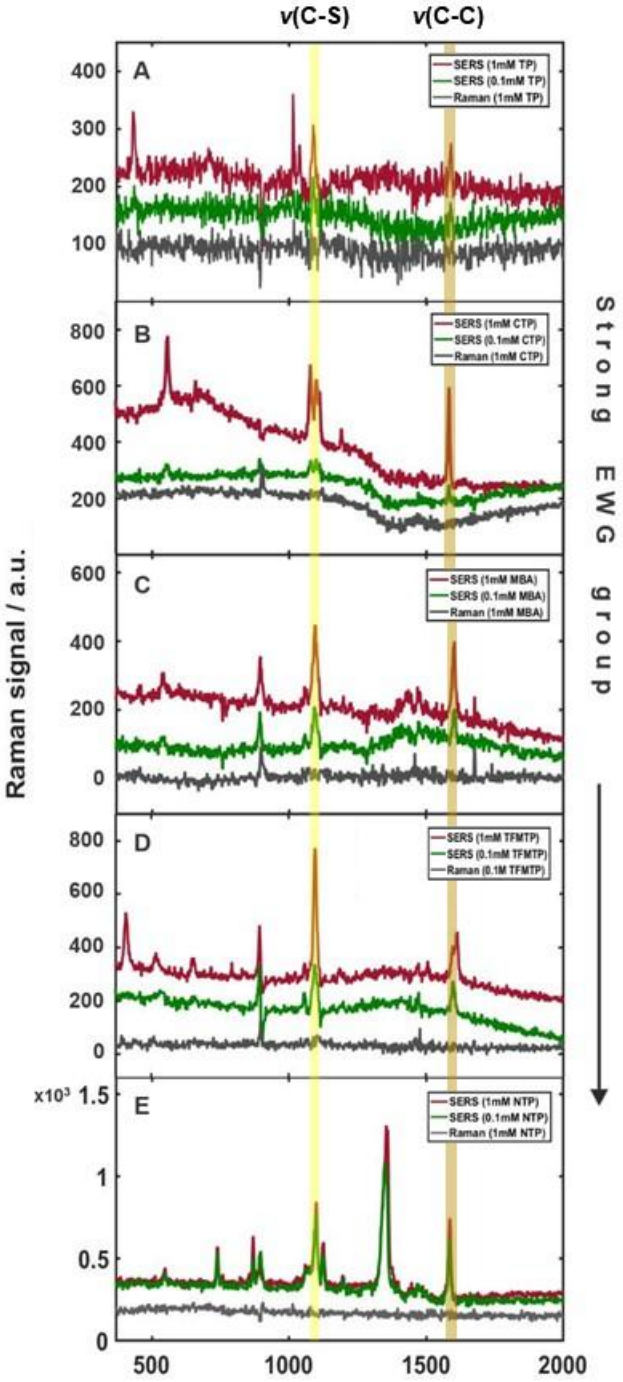

Figure 14. SERS spectra with EWGs that are TP (A), CTP (B), MBA (C), TFMTP (D), NTP (E)

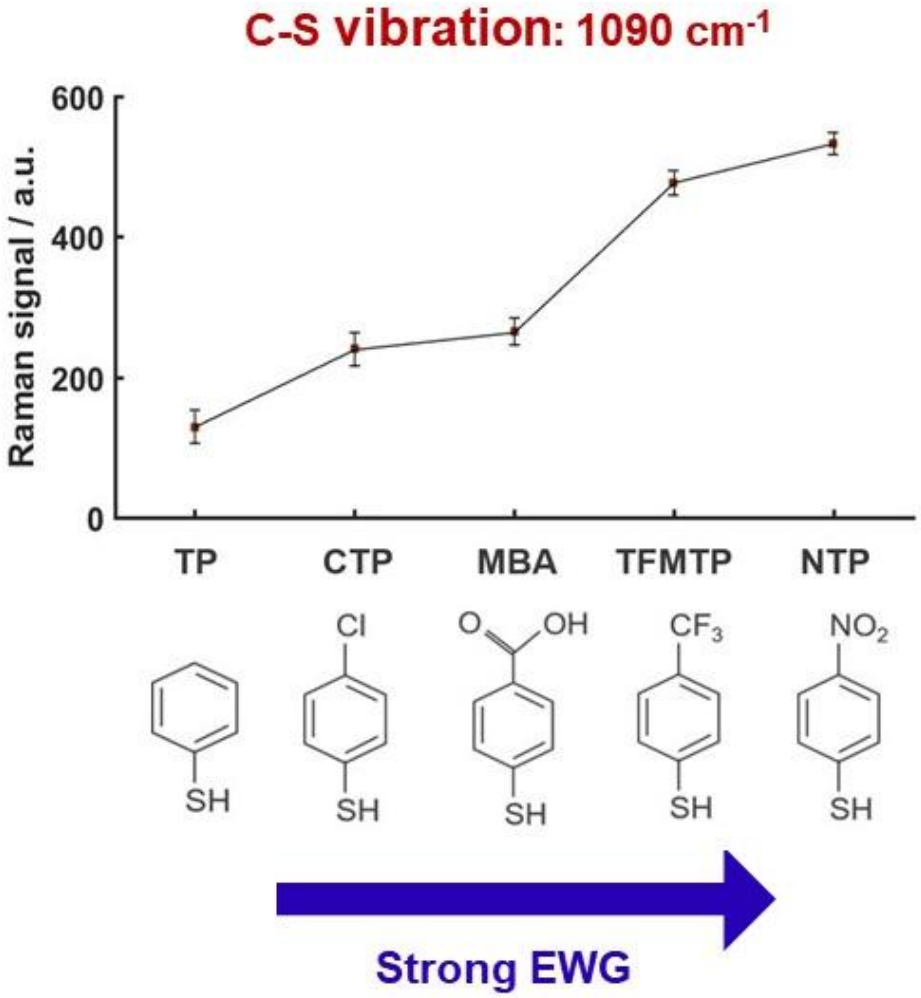

Figure 15. The relative Raman intensities of EWGs spectra with a peak in 1090 cm^{-1}, assigned to C-S vibration. The results show SERS enhancement is proportional to the strength of withdrawing force

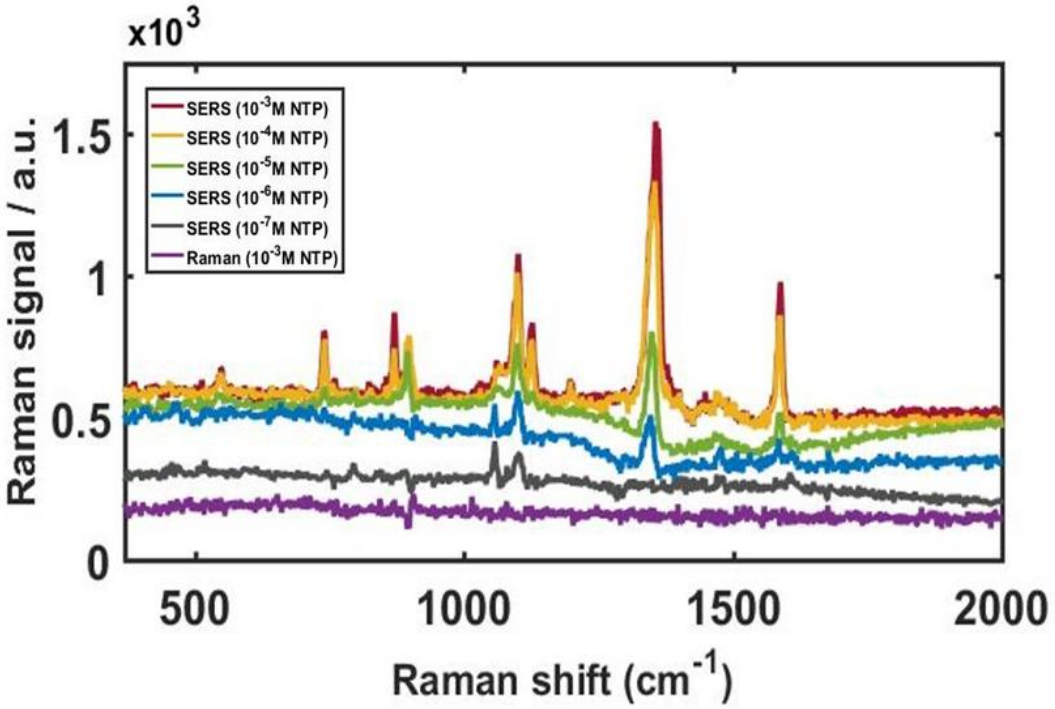

Figure 16. SERS spectrum of NTP with the lower concentration up to 100 nM, indicating the powerful enhancement

III-2-4. Electron donating group effect

To investigate the effect of EDGs, ATP with the strongest group and the next strong MP are studied, presented in figure 17A. According to our assumption that electrophilicity of substitutions is a major factor for the charge-transfer and withdrawing force could help the progress, SERS with EDGs should be weak enhancement but the result shows different behavior, that even the stronger ATP is higher than MP indicated in figure 17B. It is certain that both EDG and EWG could make the larger change of polarizability than the standard substituent, hydrogen (-H), such as TP and there could be some enhancement connected with Raman selection rules. But more detailed explanation needs to interpret the results enough and we suggest several possible directions to explain it from this unexpected result. First, we consider the possibility of intermolecular interaction between probe molecules like dimerization with hydrogen bonding of cysteamine known widely. When the adsorbed molecules interact each other through possible hydrogen bonding with amino group ($-NH_2$) of ATP and hydroxy group (-OH) of MP, the formed SAMs system can approach each other, like aggregation, making almost hot-spots between these system as shown in scheme 5A.[39] This explanation is convincing with the point that the most enhanced peaks in figure 17A are related with "a_1 mode" known as the evidence of EM enhancement. This means the electromagnetically enhanced factors could affect and support the presence of hot-spot through intermolecular interaction.

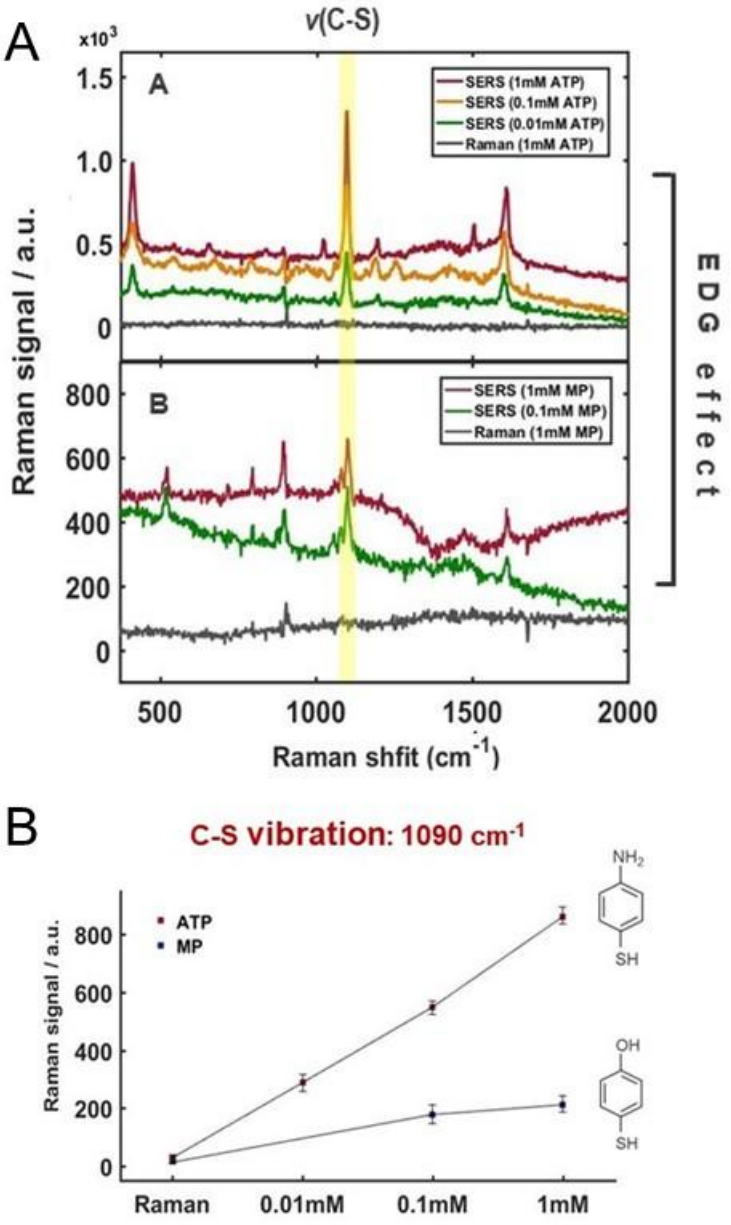

Figure 17. SERS spectra with ATP and MP at various concentration (1 mM, 0.1 mM, 0.01 mM) and normal Raman spectrum at 1 mM (A), Raman and SERS signal intensity of the vibrational mode υ(C-S) versus various concentrations (B)

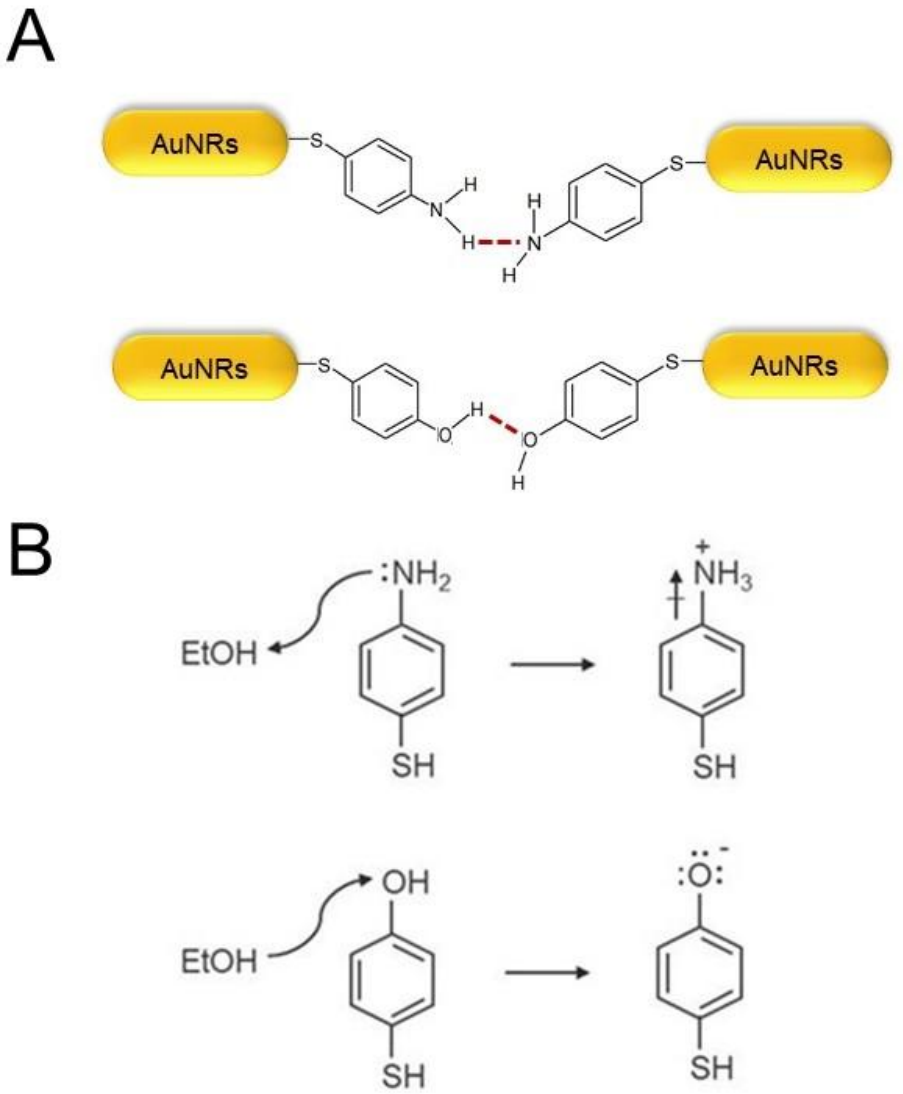

Scheme 5. Proposed structural forms affected enhancement of EDG molecules. Formation of aggregations through intermolecular interaction, hydrogen bonding between SAMs (A), the effect of solvent, ethanol in ATP and MP (B)

Also, there is an experimental evidence about this feasibility of this forms with UV-Vis spectrum and DF images in figure 18 and figure 19. UV-Vis spectrum shows even the concentration of AuNRs in samples is set equally, when the EDG molecules are adsorbed on gold, the LSPR peaks in longitudinal show red-shift and become broad with decreasing intensities indicating the distinct feature of the aggregation. But EWG molecule, NTP shows almost constant LSPR peak, especially longitudinal mode and rare broadening. The loss of intensity compared with raw AuNRs is caused by centrifugation. Also, in DF images in figure 19, we compared behavior of ATP and NTP in solution. With ATP, there is a tendency to aggregate AuNRs with the intense signals and slow movement of spots. Otherwise, NTP that has low possibility of intermolecular interaction due to the absence of hydrogen in substituent indicated almost single nanoparticle or small aggregations unlike ATP. From these data, it is demonstrated that EDG behaves differently with EWG. But this approach is incomplete because the benzene ring causes resonance forms with radiation source resulting interrupting intermolecular interactions following the change state of substituent and hydrogen bonding between hydroxy group is stronger than amino group but the ATP that has an amino group shows higher enhancement. The effect of intermolecular interaction must not be overlooked with some evidences, but it isn't the dominant explanation for the result and there is certainly another factor.

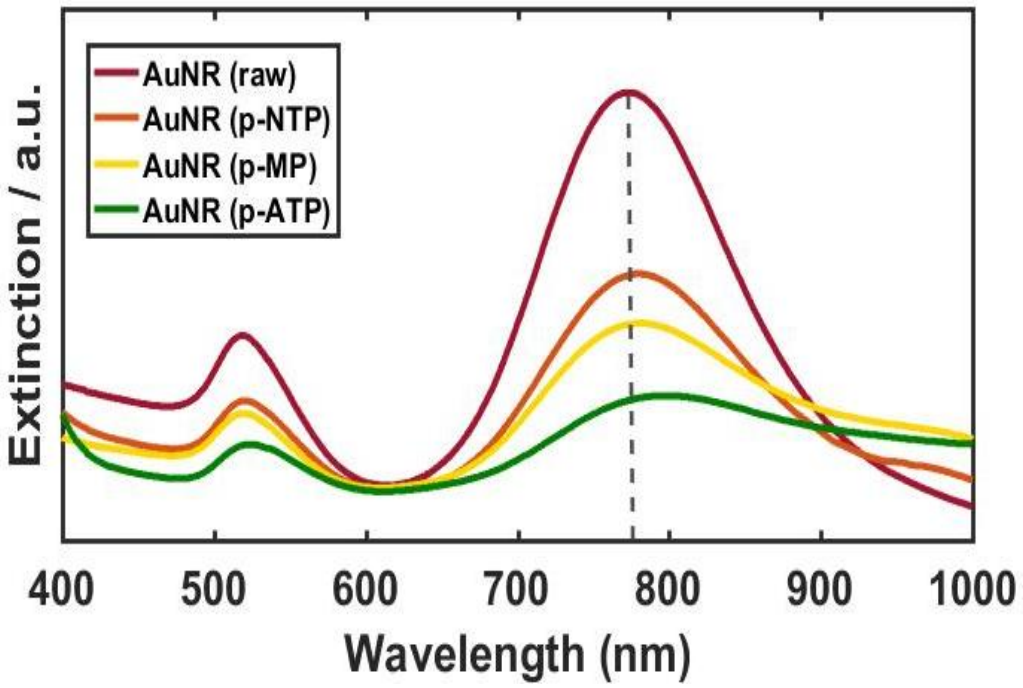

Figure 18. UV-Vis spectra of raw AuNRs (red line), NTP adsorbed AuNRs (orange line), MP adsorbed AuNRs (yellow line) and ATP adsorbed AuNRs (green line), showing red-shift with decreasing intensity and weak broadening in case of EDGs

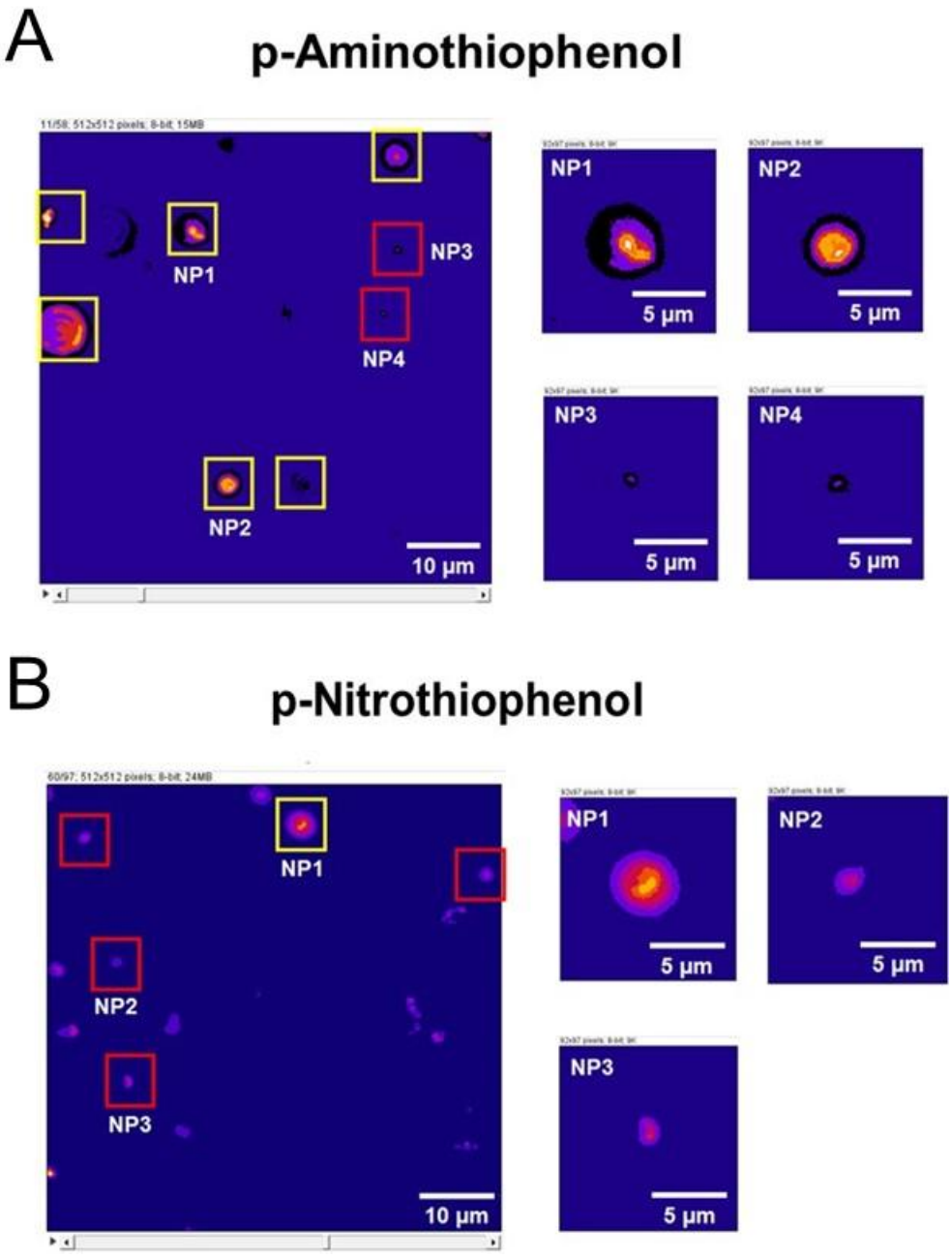

Figure 19. DF images of SERS sample with ATP in solution. There are aggregations of AuNRs showing the more intense, brighter and bigger spots in images (A), DF images of SERS sample with NTP in solution. Most signals indicate single particle or small aggregations (B)

Next, we combine the experimental result with the effect of solvent, ethanol.[38] When the lone pair of amino group of ATP interact with ethanol, amino group ($-NH_2$) could be the positive charge ($-NH_3^+$) with accepting hydrogen from ethanol and this form could be withdrawing electrons from benzene ring temporarily and act like EWG as shown in scheme 5B. This approach is also possible considering higher acid dissociation constant (pK_a) of aniline derivative. But MP cannot form this system like ATP with low pK_a and even if this reaction is possible, substituent of MP remains negative charge, finally EDG, explaining the SERS data reasonably. To demonstrate this approach, we repeat EDG experiment the same condition with different solvent, dimethyl sulfoxide (DMSO) and tetrahydrofuran (THF) that cannot donate hydrogen to probe molecules. Without hydrogen donating to ATP, it cannot form a positive charge with behavior like EWG. As a result, figure 20 shows the lower enhancement appear in different solvent, corresponding our expected result, supporting our approach enough. LSPR of gold nanoparticle can be changed with refractive index of surrounding material, affecting the resonance condition in SERS. DMSO has higher values than ethanol that means the change of EM effect, LSPR shift of AuNRs, close to 785 nm but THF that has similar refractive index of 1.4 with ethanol of 1.37 is more reasonable to compare in simliar EM condition and show the lowest SERS enhancement. From these two approaches, in case of EDG, the enhancement cannot be explained with only CE mechanism simply, but meaningful in understanding CE in SERS completely.

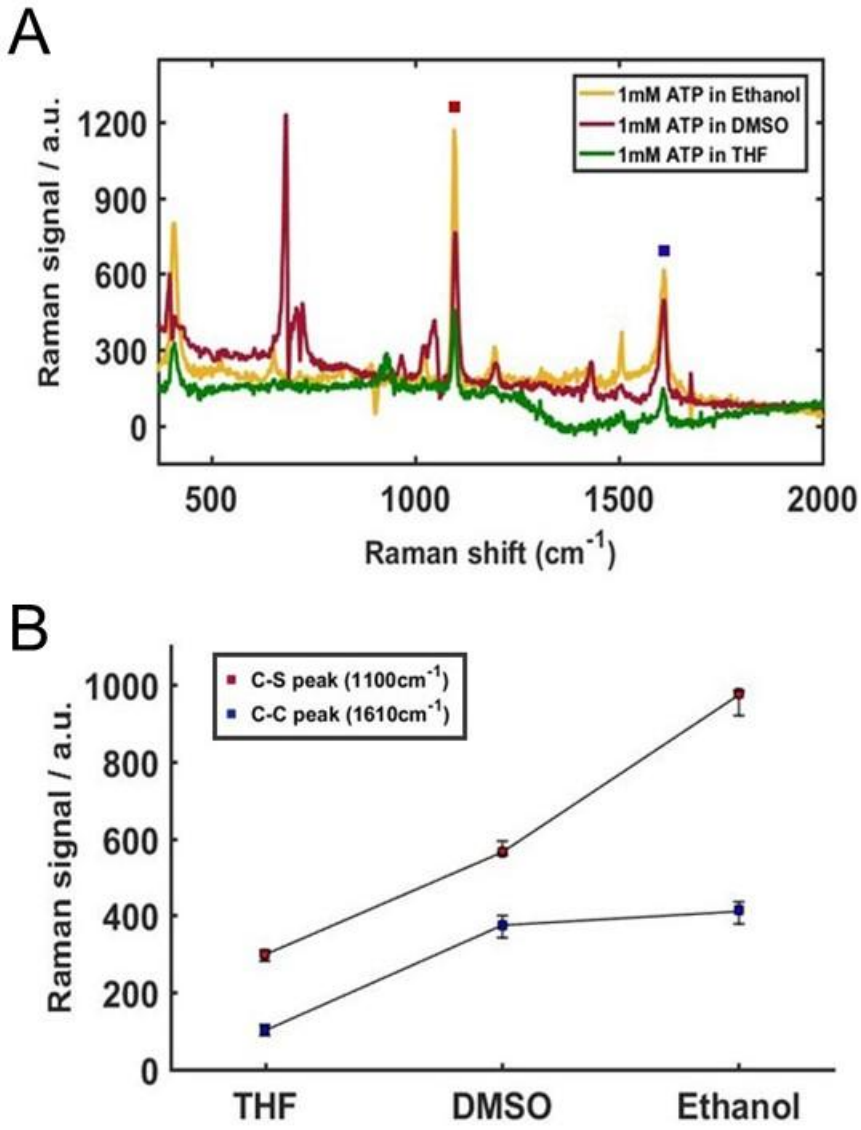

Figure 20. SERS spectrum of ATP with different solvents that are not capable of proton donation to probe molecules. Standard peaks for the comparison are 1090 cm^{-1} assigned to C-S vibration and 1610 cm^{-1} with C-C vibration. (A), The intensities of SERS standard peaks are plotted with the solvent effect (B)

III-2-5. Enhancement factor calculation[40]

Enhancement factor (EF) indicates the magnitude of signal amplification purely with the following expression. EF is meaningful to compare the enhancement with different condition of similar experiment.

$$EF = \frac{I_{SERS} / N_{SERS}}{I_{NRS} / N_{NRS}}$$

I_{SERS} : Intensity of SERS signal

N_{SERS} : Number of molecules in SERS

I_{NRS} : Intensity of normal Raman signal

N_{NRS} : Number of molecules in normal Raman

The factors related with intensities, I_{SERS} and $I_{NRS,}$ could be obtained from the SERS and Raman spectrum simply, but the number of molecules in system is hard to know exactly. We assume the samples are homogeneous uniformly and the molecules adsorbed are packed densely with monolayer. $N_{NRS,}$ number of molecules in normal Raman sample, is estimated ideally with capillary tube and N_{SERS} meaning the number of molecules adsorbed on AuNRs is calculated with the method followed.[41]

$$\mathbf{N_{SERS} = N_d A_{laser} A_N / \sigma}$$

N_d indicates the number density of the gold nanoparticles, A_{laser} is the focal spot area of laser, A_N is the footprint area of the gold nanoparticles, and σ means the surface area occupied by a single adsorbed probe molecule.

Firstly, to obtain $N_{NRS,}$ the focal laser spot is calculated with the slit width, 100 μm and the capillary tube with the inner diameter, 0.8 mm. The volume of the capillary tube within the red zone in figure S16 regard as the laser spot, 0.05 nm^3. The concentration of sample is 1 mM and the number of molecules in laser spot can be obtained with Avogadro number, estimated about 3.01 x 10^{13}.

For the factor, $N_{SERS,}$ the number of density of gold nanoparticles (N_d) is determined by the concentration of stock solution purchased from Sigma aldrich (St. Louis, MO, USA), 6.72x10^{10} /mL and the total volume of SERS samples is 200 μL, with the ideal shape of figure 21 determined with SEM images, about 7810 nm^2. Finally, the surface area occupied by an adsorbed probe molecule (σ) is obtained from several reference from 0.3 nm^2 to 0.5 nm^2/molecule.[42-44]

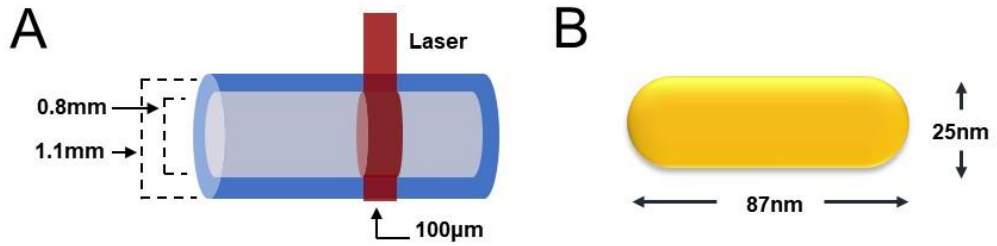

Figure 21. The ideal model of the focal spot of laser and surface area of AuNRs for calculated factors for enhancement factor calculation

The intensities of Raman and SERS are collected from the C-S vibration in 1090 cm^{-1} and the C-C ring vibration in 1590 cm^{-1}, respectively and the value of EFs are shown in Table 1.

Probe molecule	EF (C-S)	EF ($C\text{-}C_{ring}$)
ThioPhenol	3.33×10^4	1.87×10^4
ChloroThioPhenol	2.06×10^5	2.07×10^5
MercaptoBenzoic Acid	1.41×10^5	2.11×10^5
TriFluoroMethylThioPhenol	1.75×10^6	2.35×10^6
NitroThioPhenol	3.33×10^6	3.31×10^6

Table 1. Enhancement factors of EWG molecules in common peaks that are C-S vibration in 1090 cm^{-1} and C-C vibration in 1590 cm^{-1}

Probe molecule	Raman (solid)	Raman (solution)	SERS	Vibrational assignment
cysteamine		688	660	ν(C-S)$_G$; gauche
	777	774	740	ν(C-S)$_T$; trans
	1031	1040	1075	ν(C-C-N)
p-ATP	385	396	407	δ(C-S)
	1088	1108	1096	ν(C-S)
	1180	1197	1195	δ(C-H)
	1497	1515	1507	ν(C-C) + δ(C-H)
	1596	1616	1609	ν(C-C)
p-MP		798	796	π(C-H)
			895	ɣ(C-H)
		1122	1100	ν(C-S) + ν(C-H) + ν(C-C)
		1628	1611	ν(C-C)
TP		432	431	ν(C-H)
		1019	1015	ν(C-C), δ(C-H)
		1110	1089	ν(C-S)
		1601	1592	ν(ring)
p-CTP			560	ν(C-Cl)
		1072	1080	ν(C-C), ν(C-S)
	1115	1115	1103	δ(C-H)
	1611	1594	1586	ν(C-C)
p-MBA	931	904	896	δ(C-O-O)
	1119	1115	1096	ν(C-S)
	1590	1614	1605	ν(C-C)
p-TFMTP		396	407	ν(C-F)
		1105	1098	ν(C-S)
		1603	1600	ν(C-C)
p-NTP	873	873	871	π(C-H)
	1096	1096	1100	ν(C-S)
	1117	1122	1126	ν(C-N)
	1348	1353	1357	ν(NO_2)
	1592	1594	1589	ν(C-C)

Table 2. Raman and SERS peak assignments for each probe molecule (ν : vibration, δ, ɣ : bending, π : wagging)[6, 36, 45-55]

III-3. Application study with cucurbit[7]urils

III-3-1. The role of cucurbit[7]urils between gold nanorods

The rigid, symmetric structure of CB[7] and its carbonyl portals can interact with gold surface effectively. We studied about the aggregation with AuNRs and CB[7]. Figure 22A shows the bulk sample contained CB[7] indicates completely colorless solution and some minute floating particles that can be seen with the naked eye while the raw AuNRs solution is reddish and clear. For the detailed observation, two different samples were measured using SEM as shown in figure 22B. It is clear that the sample with CB[7] formed aggregations that were much compact condition and contained more nanoparticles in the range of SEM images compared with the sample without CB[7], raw AuNRs. Even the images with smaller magnification (right) indicated the much evident tendency of aggregation clearly with the wider view. Also, figure 23 indicated UV-Vis spectra with same results. We compared three type of samples that was raw AuNRs (A), centrifuged AuNRs (B) that this step had a possibility to cause broadening due to removal of surfactant that protect the surface and shape of AuNPs, and AuNRs added CB[7] (C). Compared with A and B, there is little broadening in longitudinal peak but the constant transverse peak in 518 nm and almost fixed position of peak of longitudinal mode (no-shift) means centrifugation don’t cause a significant effect. However, C in figure 23C showed the change of both mode, longitudinal and transverse peaks. In longitudinal mode, the peak showed

large broadening with small shoulder peak and clear red-shift over 900 nm. Also, transverse peak indicated relatively small proportion with the decrease of intensity. From these data, it is demonstrated that AuNPs can form aggregation easily with the presence of CB[7].

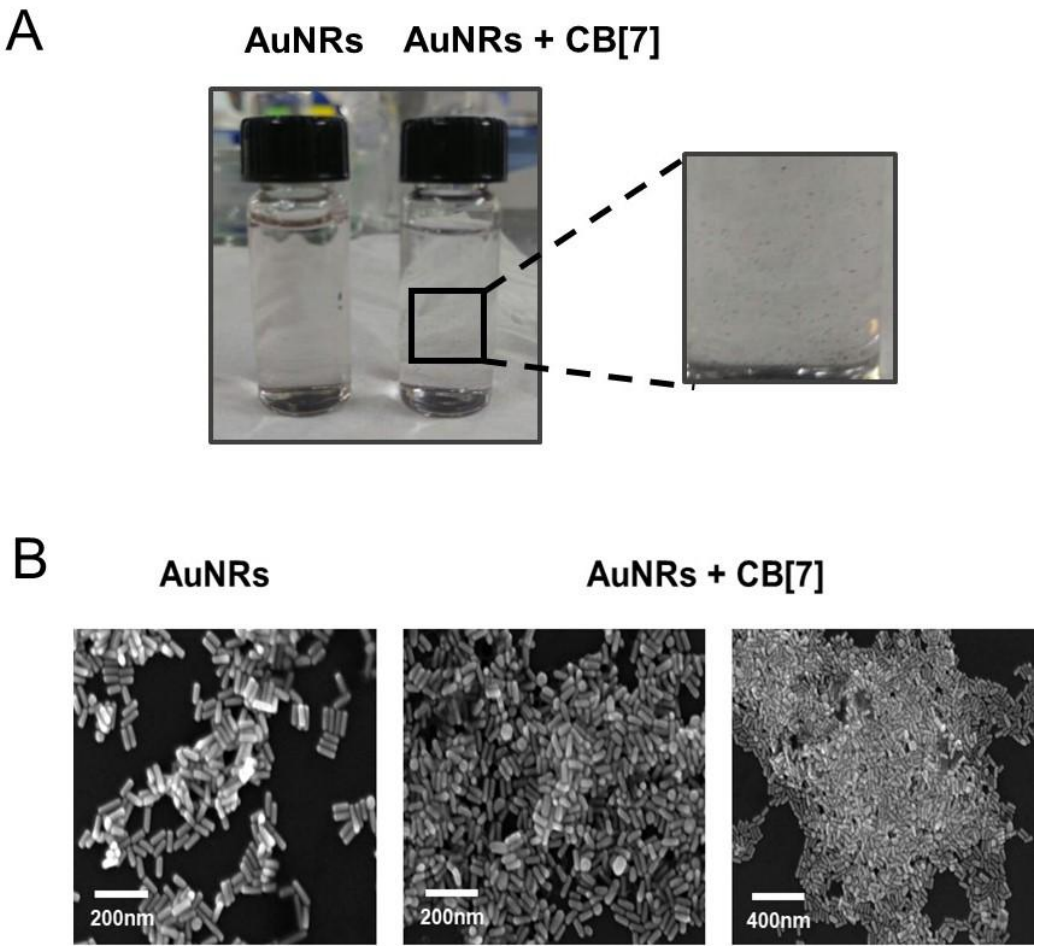

Figure 22. Photographs of pure AuNRs solution and one with CB[7] (A), SEM images of AuNRs with CB[7] and without CB[7] (B)

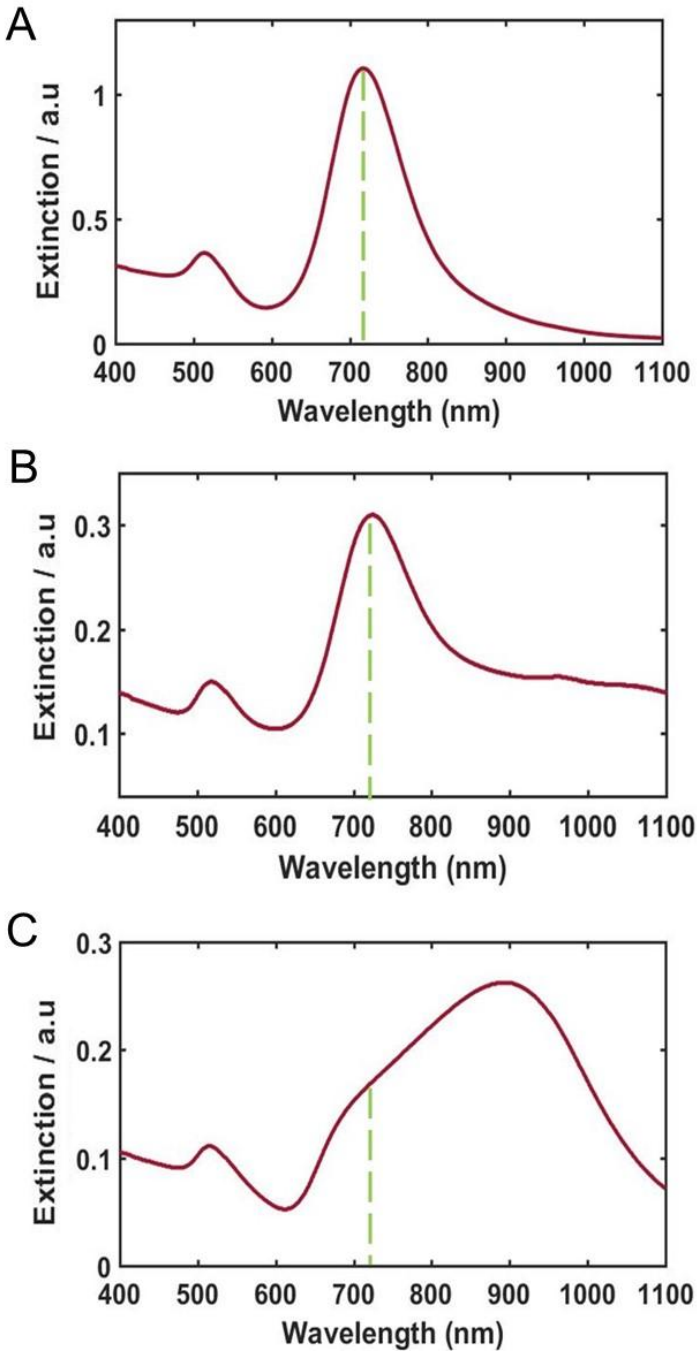

Figure 23. UV-Vis extinction spectrum of CTAB capped-AuNRs solution (A), centrifugated AuNRs solution (B), AuNRs solution with CB[7] (C)

III-3-2. SERS with long-term stability

The host-guest interaction between electron-rich CB[7] and relatively electron-deficient R6G can cause the encapsulation of R6G inside CB[7] effectively.[56] We studied the potential of CB[7] as a SERS container that keep the enhanced signals, focusing stability. From our previous study, R6G showed effective binding with AuNUs through its positive nitrogen but there was certain binding time, resulting in decreasing of enhancement after 8 hours. This means there is no doubt R6G molecule to interact with AuNPs with low stability. We compared two condition with SERS effect as shown in scheme 7, expecting that the encapsulation could be helpful to constant enhancement through the interaction with AuNPs and CB[7], even indirect interaction with R6G. Figure 24 shows the results with SERS spectra. In normal SERS, with just AuNRs and R6G as shown in figure 24A, the enhanced signals weaken over time and even after 20 days, there is rarely distinguishable peaks in the spectrum. Meanwhile, figure 24B indicates SERS spectrum in case of the presence of CB[7] as the container. By the encapsulation of R6G inside CB[7], the enhancement is not only powerful as much as figure 24A but also isn't significantly influenced by the flow of time showing the constant enhanced peaks up to 20 days. These results suggest the information about the potential of generalization in SERS even the molecule not to interact with metal surface, showing the quite well with direct interaction with similar enhancement and long-term stability.

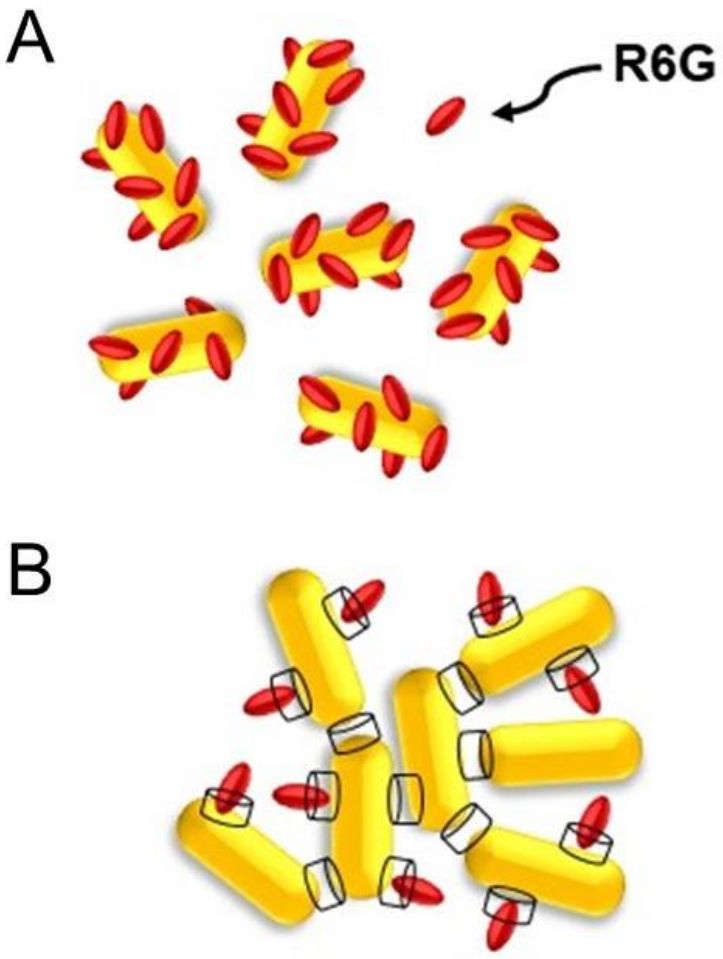

Scheme 7. Scheme of two different SERS sample, mixture of AuNRs and R6G (A), AuNRs with encapsulation of R6G in CB[7] (B)

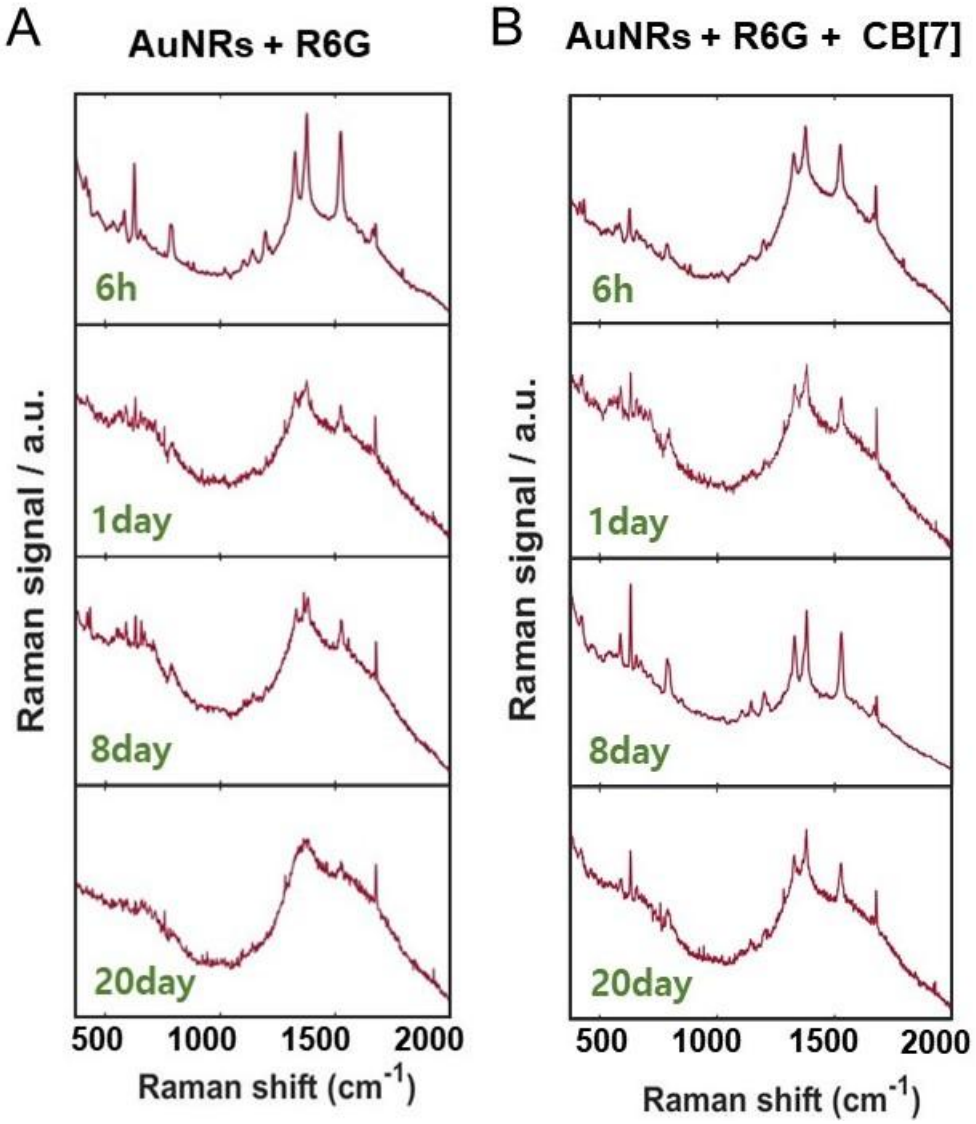

Figure 24. SERS spectra with the time from 6 hours to 20 days without CB[7] (A), with CB[7] (B)

IV. Conclusion

In conclusion, we studied SERS focused from fundamental to application. First, we investigated several factors that affected the enhancement of SERS using 100 nm branched AuNUs and R6G as probe molecules, measured at 785 nm excitation, close to their LSPR wavelength. The enhancement in SERS was effectively achieved at a AuNU:R6G concentration ratio of 8:1, a binding time of 6–8 h, centrifuging conditions of 2400 rcf for 40 min, and no stirring step during sample preparation. Therefore, the results provide important information on effective adsorption of R6G Raman probe molecules on the branched and uneven surfaces of AuNUs for effective enhancement of SERS.

Second, we have systematically studied about SERS with AuNRs and diverse substituted-thiophenols for elucidating chemical effect with We demonstrated the benzene ring could enhance signals effectively through its conjugation aromatic ring, whereas the carbon chain showed obviously weak results, with comparing SERS in cysteamine and ATP. With EWG study, it is revealed stronger EWGs in para-thiophenol causes powerful enhancements related with charge-transfer, obtaining enhancement factor up to $10^{4\sim6}$. But, EDG can show enough enhancement but this affect with several factors such as intermolecular interaction and an effect of solvent, not CE purely. This study could be useful for understanding the chemical mechanism for SERS, relatively less studied and expanding the deep approach in theory of SERS.

Finally, we investigated about the aggregation with AuNRs and CB[7] as bridge molecules. There is no doubt that CB[7] can form aggregations of AuNRs s spontaneously based on three evidences that are the bulk sample that showed colorless solution with minute particles visible to the naked eye, the SEM images with densely positioning AuNRs, much nanoparticles in the range compared with the absence of CB[7] and UV-Vis spectra compared these samples. Also, CB[7] shows high potential as sample containers resulting in long-term stability up to 20 days with the constant and enough enhancement of SERS. The molecules that have been hard to apply for SERS due to low binding ability on metal surface or insolubility can be introduced SERS with the CB[7].

V. Reference

1. Fleischmann, M.; Hendra, P. J.; McQuillan, A. J., Raman spectra of pyridine adsorbed at a silver electrode. *Chemical Physics Letters* **1974,** *26* (2), 163-166.
2. Kneipp, K.; Wang, Y.; Kneipp, H.; Perelman, L. T.; Itzkan, I.; Dasari, R. R.; Feld, M. S., Single molecule detection using surface-enhanced Raman scattering (SERS). *Physical review letters* **1997,** *78* (9), 1667.
3. Nie, S.; Emory, S. R., Probing single molecules and single nanoparticles by surface-enhanced Raman scattering. *science* **1997,** *275* (5303), 1102-1106.
4. Radziuk, D.; Moehwald, H., Highly effective hot spots for SERS signatures of live fibroblasts. *Nanoscale* **2014,** *6* (11), 6115-6126.
5. Billmann, J.; Otto, A., Experimental evidence for a local mechanism of surface enhanced Raman scattering. *Applications of Surface Science* **1980,** *6* (3-4), 356-361.
6. Bloxham, S.; Eicher Lorka, O.; Jakubėnas, R.; Niaura, G., Adsorption of Cysteamine at Copper Electrodes as Studied by Surface Enhanced Raman Spectroscopy. *Spectroscopy letters* **2003,** *36* (3), 211-226.
7. Schatz, G. C.; Young, M. A.; Van Duyne, R. P., Electromagnetic mechanism of SERS. In *Surface-enhanced Raman scattering*, Springer: 2006; pp 19-45.
8. Yamada, H.; Nagata, H.; Toba, K.; Nakao, Y., Charge-transfer band and SERS mechanism for the pyridine-Ag system. *Surface science* **1987,** *182* (1-2), 269-286.
9. Kleinman, S. L.; Frontiera, R. R.; Henry, A.-I.; Dieringer, J. A.; Van Duyne, R. P., Creating, characterizing, and controlling chemistry with SERS hot spots. *Physical Chemistry Chemical Physics* **2013,** *15* (1), 21-36.
10. Benz, F.; Chikkaraddy, R.; Salmon, A.; Ohadi, H.; de Nijs, B.; Mertens, J.; Carnegie, C.; Bowman, R. W.; Baumberg, J. J., SERS of individual nanoparticles on a mirror: size does matter, but so does shape. *The journal of physical chemistry letters* **2016,** *7* (12), 2264-2269.

11. Fan, M.; Lai, F.-J.; Chou, H.-L.; Lu, W.-T.; Hwang, B.-J.; Brolo, A. G., Surface-enhanced Raman scattering (SERS) from Au: Ag bimetallic nanoparticles: the effect of the molecular probe. *Chemical Science* **2013,** *4* (1), 509-515.

12. Rycenga, M.; Xia, X.; Moran, C. H.; Zhou, F.; Qin, D.; Li, Z. Y.; Xia, Y., Generation of Hot Spots with Silver Nanocubes for Single Molecule Detection by Surface Enhanced Raman Scattering. *Angewandte Chemie* **2011,** *123* (24), 5587-5591.

13. Seo, M.; Ha, J. W., Effective surface-enhanced Raman scattering of randomly branched gold nano-urchins with Rhodamine 6G as Raman reporters. *Microchemical Journal* **2018,** *140*, 47-51.

14. Taylor, R. W.; Lee, T.-C.; Scherman, O. A.; Esteban, R.; Aizpurua, J.; Huang, F. M.; Baumberg, J. J.; Mahajan, S., Precise subnanometer plasmonic junctions for SERS within gold nanoparticle assemblies using cucurbit [n] uril "glue". *Acs Nano* **2011,** *5* (5), 3878-3887.

15. Campion, A.; Kambhampati, P., Surface-enhanced Raman scattering. *Chemical society reviews* **1998,** *27* (4), 241-250.

16. Lombardi, J. R.; Birke, R. L.; Lu, T.; Xu, J., Charge transfer theory of surface enhanced Raman spectroscopy: Herzberg–Teller contributions. *The Journal of chemical physics* **1986,** *84* (8), 4174-4180.

17. Suzuki, M.; Niidome, Y.; Terasaki, N.; Inoue, K.; Kuwahara, Y.; Yamada, S., Surface-enhanced nonresonance Raman scattering of rhodamine 6G molecules adsorbed on gold nanorod films. *Japanese journal of applied physics* **2004,** *43* (4B), L554.

18. Aizpurua, J.; Bryant, G. W.; Richter, L. J.; De Abajo, F. G.; Kelley, B. K.; Mallouk, T., Optical properties of coupled metallic nanorods for field-enhanced spectroscopy. *Physical Review B* **2005,** *71* (23), 235420.

19. Wang, Z.; Mohamed, M.; Link, S.; El-Sayed, M., Crystallographic facets and shapes of gold nanorods of different aspect ratios. *Surface Science* **1999,** *440* (1-2), L809-L814.

20. Chen, A.; DePrince, A. E.; Demortière, A.; Joshi Imre, A.; Shevchenko, E.

V.; Gray, S. K.; Welp, U.; Vlasko Vlasov, V. K., Self Assembled Large Au Nanoparticle Arrays with Regular Hot Spots for SERS. *Small* **2011,** *7* (16), 2365-2371.

21. Wang, H.; Levin, C. S.; Halas, N. J., Nanosphere arrays with controlled sub-10-nm gaps as surface-enhanced Raman spectroscopy substrates. *Journal of the American Chemical Society* **2005,** *127* (43), 14992-14993.

22. Lee, T.-C.; Scherman, O. A., Formation of dynamic aggregates in water by cucurbit [5] uril capped with gold nanoparticles. *Chemical Communications* **2010,** *46* (14), 2438-2440.

23. Baia, M.; Toderas, F.; Baia, L.; Popp, J.; Astilean, S., Probing the enhancement mechanisms of SERS with p-aminothiophenol molecules adsorbed on self-assembled gold colloidal nanoparticles. *Chemical Physics Letters* **2006,** *422* (1-3), 127-132.

24. Fleger, Y.; Mastai, Y.; Rosenbluh, M.; Dressler, D., SERS as a probe for adsorbate orientation on silver nanoclusters. *Journal of Raman Spectroscopy* **2009,** *40* (11), 1572-1577.

25. Hildebrandt, P.; Stockburger, M., Surface-enhanced resonance Raman spectroscopy of Rhodamine 6G adsorbed on colloidal silver. *The Journal of Physical Chemistry* **1984,** *88* (24), 5935-5944.

26. Song, H. M.; Deng, L.; Khashab, N. M., Intracellular surface-enhanced Raman scattering (SERS) with thermally stable gold nanoflowers grown from Pt and Pd seeds. *Nanoscale* **2013,** *5* (10), 4321-4329.

27. Liu, Y.; Yuan, H.; Fales, A. M.; Vo Dinh, T., pH sensing nanostar probe using surface enhanced Raman scattering (SERS): theoretical and experimental studies. *Journal of Raman Spectroscopy* **2013,** *44* (7), 980-986.

28. Wang, Y.; Wang, Y.; Wang, W.; Sun, K.; Chen, L., Reporter-embedded SERS tags from gold nanorod seeds: selective immobilization of reporter molecules at the tip of nanorods. *ACS applied materials & interfaces* **2016,** *8* (41), 28105-28115.

29. Li, B.; Zhang, W.; Chen, L.; Lin, B., A fast and low cost spray method for prototyping and depositing surface enhanced Raman scattering arrays on

microfluidic paper based device. *Electrophoresis* **2013,** *34* (15), 2162-2168.

30. Schwartzberg, A. M.; Grant, C. D.; Wolcott, A.; Talley, C. E.; Huser, T. R.; Bogomolni, R.; Zhang, J. Z., Unique gold nanoparticle aggregates as a highly active surface-enhanced Raman scattering substrate. *The Journal of Physical Chemistry B* **2004,** *108* (50), 19191-19197.

31. Kitching, H.; Kenyon, A. J.; Parkin, I. P., The interaction of gold and silver nanoparticles with a range of anionic and cationic dyes. *Physical Chemistry Chemical Physics* **2014,** *16* (13), 6050-6059.

32. Wang, Y.; Yan, B.; Chen, L., SERS tags: novel optical nanoprobes for bioanalysis. *Chemical reviews* **2012,** *113* (3), 1391-1428.

33. Zhang, W.; Li, B.; Chen, L.; Wang, Y.; Gao, D.; Ma, X.; Wu, A., Brushing, a simple way to fabricate SERS active paper substrates. *Analytical Methods* **2014,** *6* (7), 2066-2071.

34. Castellana, E. T.; Gamez, R. C.; Gómez, M. E.; Russell, D. H., Longitudinal surface plasmon resonance based gold nanorod biosensors for mass spectrometry. *Langmuir* **2010,** *26* (8), 6066-6070.

35. Zijlstra, P.; Chon, J. W.; Gu, M., Five-dimensional optical recording mediated by surface plasmons in gold nanorods. *nature* **2009,** *459* (7245), 410.

36. Kudelski, A.; Hill, W., Raman study on the structure of cysteamine monolayers on silver. *Langmuir* **1999,** *15* (9), 3162-3168.

37. Huang, Y.-F.; Wu, D.-Y.; Zhu, H.-P.; Zhao, L.-B.; Liu, G.-K.; Ren, B.; Tian, Z.-Q., Surface-enhanced Raman spectroscopic study of p-aminothiophenol. *Physical Chemistry Chemical Physics* **2012,** *14* (24), 8485-8497.

38. Zhang, D.; Liang, P.; Yu, Z.; Huang, J.; Ni, D.; Shu, H.; Dong, Q.-m., The effect of solvent environment toward optimization of SERS sensors for pesticides detection from chemical enhancement aspects. *Sensors and Actuators B: Chemical* **2018,** *256*, 721-728.

39. Wang, Y.; Zhao, B.; Ozaki, Y., Exploring the Effect of Intermolecular Hydrogen Bonding and the Application in Label-Free Enantioselective Discrimination by SERS. In *Frontiers of Plasmon Enhanced Spectroscopy Volume 1*,

ACS Publications: 2016; pp 109-130.

40. Jia, H.; Bai, X.; Li, N.; Yu, L.; Zheng, L., Siloxane surfactant induced self-assembly of gold nanoparticles and their application to SERS. *CrystEngComm* **2011,** *13* (20), 6179-6184.

41. Orendorff, C. J.; Gearheart, L.; Jana, N. R.; Murphy, C. J., Aspect ratio dependence on surface enhanced Raman scattering using silver and gold nanorod substrates. *Physical Chemistry Chemical Physics* **2006,** *8* (1), 165-170.

42. Huang, J.; Zhu, Y.; Lin, M.; Wang, Q.; Zhao, L.; Yang, Y.; Yao, K. X.; Han, Y., Site-specific growth of Au–Pd alloy horns on Au nanorods: a platform for highly sensitive monitoring of catalytic reactions by surface enhancement raman spectroscopy. *Journal of the American Chemical Society* **2013,** *135* (23), 8552-8561.

43. Sergiienko, S.; Moor, K.; Gudun, K.; Yelemessova, Z.; Bukasov, R., Nanoparticle–nanoparticle vs. nanoparticle–substrate hot spot contributions to the SERS signal: studying Raman labelled monomers, dimers and trimers. *Physical Chemistry Chemical Physics* **2017,** *19* (6), 4478-4487.

44. Sisco, P. N.; Murphy, C. J., Surface-coverage dependence of surface-enhanced raman scattering from gold nanocubes on self-assembled monolayers of analyte. *The Journal of Physical Chemistry A* **2009,** *113* (16), 3973-3978.

45. Abdelsalam, M., Surface enhanced raman scattering of aromatic thiols adsorbed on nanostructured gold surfaces. *Open Chemistry* **2009,** *7* (3), 446-453.

46. Holze, R., The adsorption of thiophenol on gold–a spectroelectrochemical study. *Physical Chemistry Chemical Physics* **2015,** *17* (33), 21364-21372.

47. Hu, X.; Wang, T.; Wang, L.; Dong, S., Surface-enhanced Raman scattering of 4-aminothiophenol self-assembled monolayers in sandwich structure with nanoparticle shape dependence: off-surface plasmon resonance condition. *The Journal of Physical Chemistry C* **2007,** *111* (19), 6962-6969.

48. Li, R.; Ji, W.; Chen, L.; Lv, H.; Cheng, J.; Zhao, B., Vibrational spectroscopy and density functional theory study of 4-mercaptophenol. *Spectrochimica Acta Part A: Molecular and Biomolecular Spectroscopy* **2014,** *122*, 698-703.

49. Li, R.; Lv, H.; Zhang, X.; Liu, P.; Chen, L.; Cheng, J.; Zhao, B., Vibrational

spectroscopy and density functional theory study of 4-mercaptobenzoic acid. *Spectrochimica Acta Part A: Molecular and Biomolecular Spectroscopy* **2015,** *148*, 369-374.

50. Mahajan, S.; Hutter, T.; Steiner, U.; Goldberg Oppenheimer, P., Tunable Microstructured surface-enhanced Raman scattering substrates via electrohydrodynamic lithography. *The Journal of Physical Chemistry Letters* **2013,** *4* (23), 4153-4159.

51. Scott, B. L.; Carron, K. T., Dynamic Raman Scattering Studies of Coated Gold Nanoparticles: 4-Mercaptopyridine, 4-Mercaptophenol, and Benzenethiol. *The Journal of Physical Chemistry C* **2016,** *120* (37), 20905-20913.

52. Taylor, C. E.; Pemberton, J. E.; Goodman, G. G.; Schoenfisch, M. H., Surface enhancement factors for Ag and Au surfaces relative to Pt surfaces for monolayers of thiophenol. *Applied spectroscopy* **1999,** *53* (10), 1212-1221.

53. Wang, P.; Li, H.; Cui, C.; Jiang, J., In situ surface enhanced Raman spectroscopy detection in high pressure solution. *Applied Surface Science* **2017,** *425*, 833-837.

54. Yamamoto, Y. S.; Kayano, Y.; Ozaki, Y.; Zhang, Z.; Kozu, T.; Itoh, T.; Nakanishi, S., Single-Molecule Surface-Enhanced Raman Scattering Spectrum of Non-Resonant Aromatic Amine Showing Raman Forbidden Bands. *arXiv preprint arXiv:1610.08270* **2016**.

55. Zhang, X.; Yu, Z.; Ji, W.; Sui, H.; Cong, Q.; Wang, X.; Zhao, B., Charge-transfer effect on surface-enhanced raman scattering (SERS) in an ordered Ag NPs/4-mercaptobenzoic acid/TiO2 system. *The Journal of Physical Chemistry C* **2015,** *119* (39), 22439-22444.

56. Martyn, T. A.; Moore, J. L.; Halterman, R. L.; Yip, W. T., Cucurbit [7] uril induces superior probe performance for single-molecule detection. *Journal of the American Chemical Society* **2007,** *129* (34), 10338-10339.